MAY. - AUG. 2024 • Volume XXV Number

THE ASEAN JOURNAL OF RADIOLOGY

Highlight

- Original Article
- Case Report
- Classic Case
- ASEAN Movement in Radiology
- Letter to the Editor and Reply

Official Journal of The

Royal College of Radiologists of Thailand

Radiological Society of Thailand

Foundation for Orphan and Rare Lung Disease

Thai Society of Vascular and Intervention Radiology

ASEAN Association of Radiology

ASEAN JOURNAL OF RADIOLOGY

ISSN 2672-9393

The ASEAN
Journal of Radiology

Editor:	*Wiwatana Tanomkiat, M.D.*
Associate Editors:	*Pham Minh Thong, M.D., Ph.D.*
	Narufumi Suganuma, M.D., Ph.D.
	Kwan Hoong Ng, Ph.D.
	Shafie Abdullah, M.D.
	Siriporn Hirunpat, M.D.
	Chang Yueh Ho, M.D.
	Maung Maung Soe, M.D.
	Kyaw Zaya, M.D.
Assistant Editor:	*Nucharin Supakul, M.D.*
Statistical Consultant:	*Alan Frederick Geater, B.Sc., Ph.D.*
Language Consultant:	*Siriprapa Saparat, EIL*
Publishing Consultant:	*Ratchada Chalarat, M.A.*
Editorial Coordinator:	*Supakorn Yuenyongwannachot, B.A., M.Sc.*
Graphics:	*Kowa Saeooi, B.A.*
Publisher:	*Foundation for Orphan and Rare Lung Disease*

CONTENTS

THE ASEAN JOURNAL OF RADIOLOGY
ISSN 2672-9393

From The Editor

Diseases, Drugs and Dust

Received 25 August 2024; accepted 25 August 2024
doi:10.46475/asean-jr.v25i2.925

According to data from the Epidemiology Division of the Ministry of Public Health, from 1 January to 20 June 2024, there were 186,900 reported flu cases resulting in 14 deaths in various regions of Thailand [1]. The first case of a new lethal variant of mpox, which the World Health Organization (WHO) termed a worldwide health crisis, was confirmed on Thailand on 21 August 2024. The affected person likely carrying the strain is a European visitor who traveled from Africa to Thailand. Although mpox has been known for decades, a new and more lethal strain known as Clade 1b has recently caused a surge in mpox cases resulting in deaths in about 3.6% of cases, with children being more susceptible, according to the WHO. Over the past few months, the surge has mainly been central to Africa with outbreaks reported in countries like the Democratic Republic of Congo, Burundi, Kenya, Rwanda, and Uganda. The Democratic Republic of Congo reported over 16,000 cases and 500 deaths from mpox this year alone. On 15 August 2024, the first case of the Clade 1 variant was confirmed outside Africa in Sweden and only 6 days later in Thailand [2].

Thailand's Ministry of Public Health has announced plans to reclassify cannabis and hemp as illegal narcotics starting 1 January 2025. Opponents of the move called for public demonstrations to protest the reclassification to keep cannabis accessible to the populace while proponents of the bill argued that the reclassification is necessary to prevent misuse and protect public health, ensuring that the plant's benefits are utilized responsibly and safely [3].

The need to protect children from the health risks associated with vaping was emphasized on 31 May, the World No Tobacco Day. According to the Southeast Asia Tobacco Control Alliance (SEATCA), five out of 10 countries in the region ban e-cigarettes. These include not only Thailand and Singapore, which have some of the strictest vaping bans in the world, but also places like Brunei, Taiwan, and Hong Kong. In Thailand, vaping has been prohibited since 2014. Possessing an e-cigarette could face fines of up to 30,000 baht in Thailand and up to 2,000 Singapore dollars in Singapore [4].

Thailand started Lung Cancer Screening (LCS) in the Regional Health-1 covering Chiang Mai, Chiang Rai, Lamphun, Lampang Nan, Phayao, and Mae Hong Son. The low-dose CT will be utilized as a screening tool and the target group includes smokers or those with family history of lung cancer aged 55-75 years old that reside in Regional Health-1 for more than 20 years. The reason to start LCS in Regional Health-1 is that there is a high prevalence of lung cancer and a high level of PM 2.5 which raise deep concerns to public that they might be related. This first organized LCS in Thailand was presented and discussed as well as recommendations, guidelines and protocols on other chest diseases among radiologists during 26-28 July 2024.

THE ASEAN JOURNAL OF RADIOLOGY
ISSN 2672-9393

Panel discussion among the expert chest radiologists on 26 July 2024

Annual conference of chest radiology during 27-28 July 2024

Wiwatana Tanomkiat, M.D.
Editor,
The ASEAN Journal of Radiology
Email: aseanjournalradiology@gmail.com

References

1. ASEANNOW.com [Internet]. The Thaiger; c 2002-2024 [cited 2024 Aug 26]. Thailand influenza outbreak: 14 deaths and over 180,000 affected. Available from: https://aseannow.com/topic/1330487-thailand-influenza-outbreak-14-deaths-and-over-180000-affected/?utm_source=240624-04

2. ASEANNOW.com [Internet]. The Thaiger; c 2002-2024 [cited 2024 Aug 26]. Thailand likely detects a new, more dangerous mpox variant. Available from: https://aseannow.com/topic/1336117-thailand-likely-detects-a-new-more-dangerous-mpox-variant/?utm_source=240822-04

3. ASEANNOW.com [Internet]. The Thaiger; c 2002-2024 [cited 2024 Aug 26]. Thailand to reclassify cannabis as illegal by 1 January, 2025. Availble from: https://aseannow.com/topic/1331767-thailand-to-reclassify-cannabis-as-illegal-by-1-january-2025/?utm_source=240708-11

4. thethaiger.com [Internet]. 2024 Jul 31 [cited 2024 Aug 26]. Vaping troubles: British tourists warned of costly holiday mistake. Available from: https://thethaiger.com/news/national/vaping-troubles-british-tourists-warned-of-costly-holiday-mistake

THE ASEAN JOURNAL OF RADIOLOGY
ISSN 2672-9393

Original Article

Findings of abdominal computed tomography in COVID-19 patients with abnormal abdominal symptoms In Siriraj Hospital

Thanawat Punyavik, M.D.
Nithida Na Songkhla, M.D.
Kobkun Muangsomboon, M.D.
From Division of Diagnostic Radiology, Department of Radiology,
Faculty of Medicine Siriraj Hospital, Mahidol University, Bangkok, Thailand.
Address correspondence to T.P. (email: thanawat1992.p@gmail.com)

Received 8 Octorber 2023; revised 1 June 2024; accepted 1 June 2024
doi:10.46475/asean-jr.v25i2.886

Abstract

Background: The coronavirus (COVID-19) is caused by the severe acute respiratory syndrome coronavirus 2 (SARS-CoV-2). Chest imaging findings of COVID-19 disease have been widely published. Only a few studies of abdominal imaging findings have been documented. The majority of these studies demonstrate thrombotic events associated with COVID-19. Previous studies were mainly conducted in the USA, Europe and China which limited the applicability in Southeast Asia (SEA) including Thailand.

Objective: To provide a summary of various abdominal imaging findings of COVID-19 patients admitted to xxx Hospital with findings associated with clinical outcomes.

Materials and methods: All CT abdominal imaging of adult patients who tested positive for COVID-19 performed from January 1st, 2020 to August 31st, 2022 were retrospectively reviewed. We collected clinical data, abdominal signs and symptoms, laboratory data and various CT findings, for example; bowel-wall thickening, bowel ischemia, fluid-filled colon and bleeding manifestations. The clinical outcomes were gathered as death confirmation, invasive mechanical ventilation, days of invasive mechanical ventilation and days of hospitalization.

Results: A large number of patients who had stage 3-5 chronic kidney disease (CKD), abdominal distension, abnormal bowel findings and longer days of hospitalization were significantly observed in a group with worse clinical outcomes. Abnormal intestinal imaging findings were related to a higher risk of worse outcomes, invasive mechanical ventilation, death and days of hospitalization without statistical significance.

Conclusion: Abdominal CT scans performed on COVID-19 patients frequently revealed abnormal bowel findings, which were strongly associated with poor clinical outcomes. Radiologists need to be concerned about abnormal bowel findings and point them out to clinicians and surgeons.

Keywords: Abdominal imaging, Abdominal symptoms, Coronavirus, COVID-19.

THE ASEAN JOURNAL OF RADIOLOGY
ISSN 2672-9393

Introduction

The coronavirus (COVID-19), caused by severe acute respiratory syndrome coronavirus 2 (SARS-CoV-2), was originally identified in China in 2019. By July 29, 2020, around 17 million people were diagnosed with coronavirus, and more than half a million people died as a consequence of this infection. Non-specific common clinical signs included flu-like symptoms like fever, coughing, exhaustion, and dyspnea [1-3]. As the number of cases expanded globally, gastrointestinal (GI) symptoms such as nausea, vomiting, diarrhea, abdominal discomfort, and lack of appetite were also noticed [4-7]. The pathophysiology of SARS-CoV-2 is well known by accessing cells via surface expression of angiotensin-converting enzyme 2 (ACE-2) [8]. ACE-2 has been found mostly in alveolar epithelial cells and the enterocytes of the small intestine and hepatobiliary cells [4, 9-11].

Chest imaging findings of COVID-19 disease have been widely published. Only a few studies of abdominal imaging findings have been documented [12-15]. The majority of these studies demonstrate thrombotic events associated with the disease, including bowel wall involvement, hepatitis, pancreatitis, gallbladder sludge, portal and upper mesenteric vein thrombosis [12-16]. Limitations of previous studies were mainly conducted in the USA, Europe and China which limited the applicability in Southeast Asia (SEA) including Thailand. The objective of this retrospective study is to provide a summary of the abdominal imaging findings of COVID-19 patients with the associated clinical outcomes.

Materials and methods

Study population

The ethics committee of Siriraj Hospital accepted our retrospective study, and the institutional review board approved it (797/2564) (IRB3). All data were collected in Siriraj Hospital which is a large quaternary care academic institution. The patient databases at the institutions relevant to COVID-19 were eventually maintained.

The inclusion criteria were adult patients, not younger than 18 years old who tested positive for COVID-19 (PCR). The patients underwent abdominal CT imaging from January 1st, 2020 to August 31st, 2022. The exclusion criteria were duplicated data and abdominal findings were associated with alternative comorbidities. The final research population consisted of fifty-nine patients.

Data collection (demographic, clinical and laboratory)

The clinical and laboratory data were collected from medical record reviews using a standardized data form. The clinical data were reviewed: age, gender and, a presence of comorbidities including diabetes, hypertension, dyslipidemia, stage 3-5 chronic kidney disease (CKD), obesity (BMI>25kg/m2), cancer and chronic lung disease (COPD, asthma). Abdominal signs and symptoms on performed abdominal CT imaging included abdominal pain, diarrhea, nausea and vomiting, abdominal distension, GI bleeding, fever with chills, hematuria, an anticoagulant drug for venous thromboembolism (VTE) prophylaxis or treatment and bleeding manifestations.

Patient outcome

Following a standardized form, a medical record review was used to obtain the clinical and laboratory data, including death confirmation, invasive mechanical ventilation and days of invasive mechanical ventilation and hospitalization. There were two groups of patients: good clinical outcomes and worse clinical outcomes. Patients who needed an intensive care unit (ICU) or died were classified as having worse clinical outcomes.

Image acquisition

A 64-slice or 256-slice CT scanner was used in all CT scans. Two patients underwent upper abdomen contrast-enhanced CT and 57 patients underwent whole abdomen contrast-enhanced CT. Images were acquired in the arterial phase (35-40 seconds following intravenous contrast injection), the portovenous phase (70–80 seconds following intravenous contrast injection). Intravenous contrast injection of 1.5-2 ml/kg of iodinated contrast (concentration 300-370 mgI/ml, Iopromide (Ultravist™), Iopamidol (Iopamiro™), Iodixanol (Visipaque™)

THE ASEAN JOURNAL OF RADIOLOGY
ISSN 2672-9393

adopted a power injector with a rate of 2–4 ml/second followed by 30 ml saline flush. Axial images were generated using a thickness of 1.25 mm and 5 mm. Five mm-thickness of sagittal and coronal reconstructions was obtained.

Imaging analysis

Independently reviewing the abdominal CT, two board-certified abdominal radiologists reached a consensus after discussing different opinions on some cases. The radiologists were blinded to clinical, treatment and outcome data. The intestinal findings were reviewed: bowel-wall thickening (small bowel, large bowel, described as a single wall thickness greater than 3 mm in distended bowel loops and greater than 5 mm in collapsed bowel loops), bowel ischemia (decreased bowel wall enhancement, vessel occlusion, and pneumatosis intestinalis/portal vein gas), intestinal perforation (a presence of peritoneal or retroperitoneal air), intestinal distension (>3 cm for small bowel and >6 cm for large bowel), a fluid-filled colon (homogeneous, low-attenuation fluid-filled bowel), solid organ infarction (hypoattenuation of organ parenchyma), pancreatitis (pancreatic edema and peripancreatic fluid), hepatitis (gallbladder wall thickening and heterogeneous liver parenchyma) and submucosal edema of the stomach. The manifestation of bleeding included intra-abdominal bleeding, retroperitoneal bleeding and abdominal wall hematoma.

Statistical analysis

SPSS (IBM SPSS Statistics for Windows, Version 28.0. Armonk, NY: IBM Corp) was employed for all statistical analyses.

Demographic and imaging data (such categorical variables as sex, comorbidities, abdominal signs and symptoms, and bleeding complications) were presented by the frequency and the percentage. Continuous variables like age, invasive mechanical days (days of invasive mechanical ventilation) and the length of stay were presented by the median and the range.

Clinical outcomes were reported as good outcomes and worse outcomes (including ICU admission and death).

The association between clinical outcomes and categorical variables (demographic, imaging data and complications) was performed by Chi-square or Fisher' Exact test and significant difference testing between clinical outcomes in continuous data such as age, invasive mechanical days (days of invasive mechanical ventilation) and the length of stay, were analyzed by Mann Whitney U-test, respectively.

For the multivariate analysis, logistic regression analysis was measured to figure out the factors for intestinal imaging findings which reported Adjusted Odd Ratio (95%CI). In case of time to event analysis, Kaplan Meier and Cox-Regression analysis were analyzed to obtain factors for an invasive mechanical ventilator, ICU admission and death events which were reported by crude and Adjusted Hazard Ratio (95%CI) and we selected the enter selection method of univariate analysis with $p<0.1$. The selection of variables for the final models is based on predetermined variables associated with COVID-19 prognosis. Statistically significant difference was regarded as a P- value lower than 0.05.

Results

All 59 patients with 59 studies were included, 34/59 (58%) were male. The average age was 65 years (ranging from 19 to 92), 59/59 (100%) were inpatients. The most frequent comorbidities were hypertension (37/59, 63%), dyslipidemia (24/59, 41%) and diabetes (21/59, 36%). For comorbidities, stage 3-5 chronic kidney disease (CKD) significantly associated with patients with worse outcomes [12/42 (29%) vs 1/17 (6%), p=0.040]. The rest of the comorbidities were not significantly different in both groups.

For abdominal signs and symptoms, the majority of the patients had fever with chills (41/59, 70%), abdominal pain (36/59, 61%) and abdominal distension (22/59, 37%). Fourteen patients (14/59, 24%) had gastrointestinal bleeding. Ten patients (10/59, 17%) had nausea and vomiting, and eight patients had hematuria (8/59, 14%). Abdominal distension was significantly associated with patients with worse outcomes. [21/42 (50%) vs 1/17 (6%), p=0.002]. Only nausea and vomiting

THE ASEAN JOURNAL OF RADIOLOGY
ISSN 2672-9393

were significantly found in patients with good outcomes. [2/42 (5%) vs 8/17 (47%), p<0.001]. Table 1 summarizes the abdominal signs and symptoms of the included patients.

Thirty-four patients (34/59, 58%) also received anticoagulant drugs for venous thromboembolism prophylaxis and treatment including enoxaparin (28/59, 47%), warfarin (3/59, 5%), fondaparinux (1/59, 2%) and bemiparin (2/59, 3%). Regarding bleeding manifestations, patients had intra-abdominal bleeding (11/59, 19%), retroperitoneal bleeding (6/59, 10%) and abdominal wall hematoma (4/59, 7%). Between good and worse outcomes, there was no significant difference in bleeding manifestations. Table 2 summarizes bleeding manifestations.

For abdominal findings on CT, the majority of patients had abnormal bowel findings (32/59, 54%) including a fluid-filled colon (27/59, 46%), colitis (14/59, 24%), small bowel thickening (4/59, 7%), intestinal perforation (3/59, 5%), bowel ischemia (2/59, 3%) and intestinal distension (2/59, 3%). Other abdominal CT findings were hepatitis (9/59, 15%), submucosal edema of the stomach (9/59, 15%), solid organ infarction (6/59, 10%) and pancreatitis (4/59, 7%). A higher proportion of patients who had abnormal bowel findings [28/42 (67%) vs 4/17 (24%), p=0.029), fluid-filled colon [25/42 (60%) vs 2/17 (12%), p=0.001] and submucosal edema of the stomach [9/42 (21%) vs 0/17 (0%), p=0.048] were significantly found in the group with worse clinical outcomes. Other abdominal findings on CT were not significantly different in both groups. Table 2 summarizes abdominal imaging features.

Considering the groups of clinical outcomes, forty-two patients had worse outcomes (42/59, 71%), including death (17/59, 29%) or being admitted to intensive care units (42/59, 71%). Thirty-four patients (34/42, 81%) with the worse outcome group were on invasive mechanical ventilators. Seventeen patients (17/59, 29%) had good clinical outcomes. Additionally, the overall days of hospitalization rate increased among patients with worse outcomes with a statistical difference [32 (3-186) vs 8 (3-74), p=0.010). Table 2 summarizes clinical outcomes of the included patients.

Table 1. *Patients' characteristics on performed abdominal CT imaging and comparison between patients with good clinical outcomes and worse clinical outcomes (intensive care unit (ICU) admission or death).*

	Number of patients N(%)	Good clinical outcome N(%)	Worse clinical outcome N(%)	P-value
Number of patients	59	17 (29%)	42 (71%)	-
Age years (range)	65	60 (19-90)	67 (28-92)	-
Male	34 (58%)	10 (59%)	24 (57%)	0.900
Female	25 (42%)	7 (41%)	18 (43%)	
Comorbidities	**Number of patients N(%)**	**Good clinical outcome N(%)**	**Worse clinical outcome N(%)**	**P-value**
Diabetes	21 (36%)	4 (23.5%)	17 (40.5%)	0.200
Hypertension	37 (63%)	8 (47%)	29 (69%)	0.100
Dyslipidemia	24 (41%)	5 (29%)	19 (45%)	0.260
Stage 3-5 chronic kidney disease (CKD)	13 (22%)	1 (6%)	12 (29%)	0.040
Obesity	8 (14%)	1 (6%)	7 (17%)	0.400
Cancer	4 (7%)	1 (6%)	3 (7%)	1
Chronic lung disease (COPD, Asthma)	7 (12%)	3 (18%)	4 (10%)	0.400

Table 1 (Continued). *Patients' characteristics on performed abdominal CT imaging and comparison between patients with good clinical outcomes and worse clinical outcomes (intensive care unit (ICU) admission or death).*

	All patients N(%)	Good clinical outcome N(%)	Worse clinical outcome N(%)	P-value
Abdominal signs and symptoms				
Abdominal pain	36 (61%)	12 (70%)	24 (57%)	0.340
Diarrhea	7 (12%)	3 (18%)	4 (10%)	0.390
Nausea and vomiting	10 (17%)	8 (47%)	2 (5%)	<0.001*
Abdominal distension	22 (37%)	1 (6%)	21 (50%)	0.002*
GI bleeding	14 (24%)	2 (12%)	12 (29%)	0.300
Fever with chills	41 (70%)	11 (64%)	30 (71%)	0.600
Hematuria	8 (14%)	2 (12%)	6 (14%)	1
On anticoagulant (Enoxaparin, Bemiparin, Warfarin, Fondaparinux)	34 (58%)	6 (35%)	28 (67%)	0.027

Table 2. *Abdominal findings on computed tomography among all patients, patients with good clinical outcomes and worse clinical outcomes (intensive care unit admission (ICU) or death).*

	Number of patients N(%)	Good clinical outcome N(%)	Worse clinical outcome N(%)	P-value
Abnormal bowel findings (included colitis, small bowel thickening, bowel ischemia, intestinal perforation, intestinal distension and a fluid-filled colon)	32 (54%)	4 (24%)	28 (67%)	0.029
• Colitis (colonic and rectal abnormalities)	14 (24%)	2 (12%)	12 (29%)	0.300
• Small bowel thickening	4 (7%)	1 (6%)	3 (7%)	1
• Bowel ischemia (decreased bowel wall enhancement, vessel occlusion, Pneumatosis intestinalis/Portal vein gas)	2 (3%)	0 (0%)	2 (5%)	1
• Intestinal perforation (presence of free peritoneal or retroperitoneal air)	3 (5%)	1 (6%)	2 (5%)	1
• Intestinal distension	2 (3%)	0 (0%)	2 (5%)	1
• Fluid-filled colon	27 (46%)	2 (12%)	25 (60%)	0.001*
Solid organ infarction	6 (10%)	1 (6%)	5 (12%)	0.660
Pancreatitis	4 (7%)	1 (6%)	3 (7%)	1
Hepatitis (GB wall thickening, heterogeneous liver parenchyma)	9 (15%)	4 (24%)	5 (12%)	0.420
Submucosal edema of stomach	9 (15%)	0 (0%)	9 (21%)	0.048
Bleeding manifestations	16 (27%)	2 (12%)	14 (33%)	0.120
Intra-abdominal bleeding	11 (19%)	2 (12%)	9 (21%)	0.500
Retroperitoneal bleeding	6 (10%)	0	6 (14%)	0.170
Abdominal wall hematoma	4 (7%)	0	4 (10%)	0.300

THE ASEAN JOURNAL OF RADIOLOGY
ISSN 2672-9393

Regarding the association between anticoagulants for VTE prophylaxis or treatment and bleeding manifestations, anticoagulants significantly increased the incidence of all bleeding manifestations (P=0.025) and retroperitoneal bleeding (P=0.034) but not significantly associated with intra-abdominal bleeding and abdominal wall hematoma. Table 3 summarizes the association between anticoagulant use for VTE prophylaxis or treatment and bleeding manifestations.

Table 3. *Association between anticoagulants for VTE prophylaxis or treatment and bleeding manifestations. The number of patients on anticoagulant for VTE prophylaxis and treatment (Enoxaparin, Bemiparin, Warfarin, Fondaparinux) = 34/59 (58%).*

	No	Yes	P-value
All bleeding manifestations	21 (49%)	13 (81%)	0.025
Intra-abdominal bleeding	26 (54%)	8 (73%)	0.300
Retroperitoneal bleeding	28 (53%)	6 (100%)	0.034
Abdominal wall hematoma	30 (55%)	4 (100%)	0.130

In regard to multivariate analysis, abnormal intestinal imaging findings were associated with a higher risk of worse outcomes without a statistical significance. (RR=1.17, p=0.646), and also longer days of hospitalization were also observed (adjusted difference: +14.3 days, p=0.103). Table 4 summarizes the association between abnormal intestinal findings on CT scan and patients' outcomes.

Additionally, ventilator free time was higher (RR=1.86, p=0.140), and survival free time was longer (RR=2.08, p=0.218) in patients without abnormal intestinal imaging findings (blue line) compared to patients with abnormal intestinal imaging findings (red line), but no statistical significance (Figure 1).

Table 4. *Association between presences of intestinal finding on computed tomography and patients' outcomes.*

	No intestinal imaging findings N(%)	Abnormal intestinal imaging findings N(%)	Crude Hazard Ratio (95% CI)	Fully adjusted Hazard Ratio* (95% CI)
Worse clinical outcome	14/27 (51.9%)	28/32 (87.5%)	RR=1.22 (0.64-2.33) P=0.553	RR=1.17 (0.60-2.26) P=0.646
Death	4/27 (15.0%)	13/32 (41.0%)	RR=1.81 (0.58-5.60) P=0.305	RR=2.08 (0.65-6.70) P=0.218
Invasive mechanical ventilation	10/27 (37.0%)	24/32 (75.0%)	RR=1.46 (0.69-3.09) P=0.318	RR=1.86 (0.82-4.24) P=0.140
	No intestinal imaging findings N(%)	**13/32 (41.0%)**	**RR=1.81 (0.58-5.60)**	**P-value**
Hospital length (days)	28.7 (28.6%)	43 (36.3%)	+14.30 (-2.98-31.56) P=0.103	1.03 (0.97-1.10) P=0.289
Invasive mechanical ventilations length (days)	33.2 (35.8%)	28.7 (31.4%)	4.53 (-29.59-20.52) P=0.715	0.96 (0.89-1.04) P=0.287

**Adjusted Odd Ratio variables associated intestinal imaging findings with p<0.1 in univariate analysis by any abdominal bleeding, GI bleeding, abdominal distension, abdominal pain, stage 3-5 CKD, respectively.*

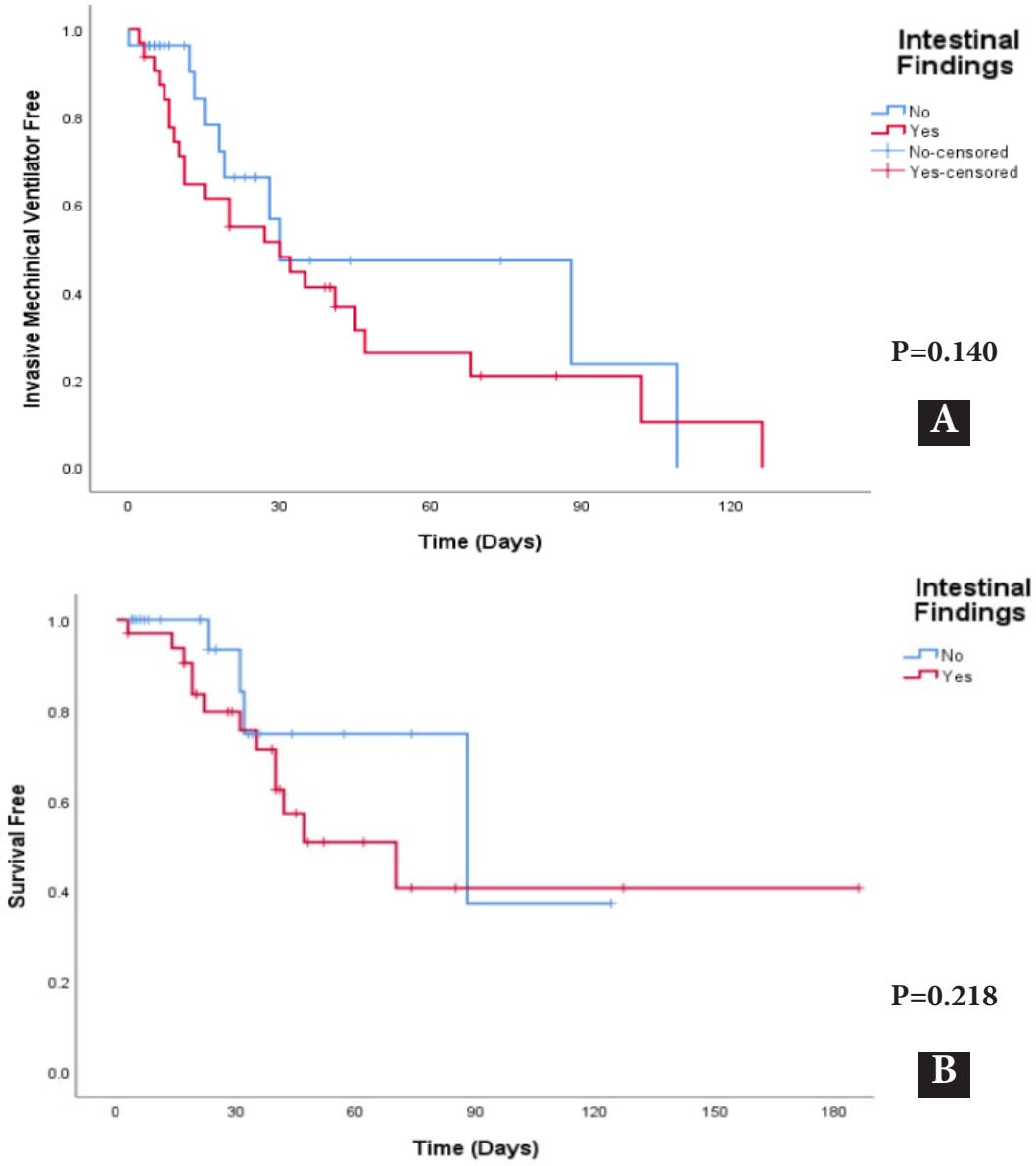

Figure 1. *Kaplan-Meier curves of invasive mechanical ventilation events (Figure A) and combined worse outcomes (Figure B), including death and invasive mechanical ventilation, comparing patients with and without intestinal imaging findings on computed tomography.*

Discussion

Coronaviruses are a group of viruses that mostly manifest with respiratory symptoms and also have extra-pulmonary effects. Involvement in the gastrointestinal tract in COVID-19 was caused by direct tissue damage and also because of inflammation-mediated cytotoxicity attributable to the strong affinity between angiotensin converting enzyme 2 (ACE2) receptor and SARS-CoV-2 [7, 9, 11, 17, 18].

Abdominal symptoms are the primary symptoms of the COVID-19 infection, such as abdominal pain, diarrhea, nausea and vomiting [4, 11, 18] also a hepato-biliary tract injury of an uncertain origin [12].

In previously published studies by Natally et al., fever with chills and abdominal pain were the 1st and 2nd most common clinical symptoms for abdominal CT scanning with 69% and 44%, respectively [9]. Similar to our study, the most common clinical symptoms were fever with chills (70%) followed by abdominal pain (61%). For nausea and vomiting which were significantly associated with good clinical outcomes were discordant with previous studies that found no significant difference in both groups [12, 19, 20]. No previous study considered abdominal distension which was significantly associated with patients with worse outcomes in our study.

In our research, for abdominal CT findings, abnormal bowel findings were significantly observed in patients with worse outcomes (P=0.029) corresponding to two previous published studies by Rajesh et al. (P=0.040) [12] and Natally et al. (P=0.03) [19] A fluid-filled colon, which possibly indicates diarrhea, was the most common CT finding (46%) which was significantly found in patients with worse outcomes (P=0.001) consistent with a previous study by Rajesh et al., which found a fluid-filled colon (43%), significantly evident in ICU patients. (P=0.01) [12]. However, inpatients with COVID-19 commonly develop gastrointestinal symptoms, including diarrhea, which might be unrecognized [5]. Although fluid-filled colons on CT scans are mostly unreported on CT images, this report could be an important clue for COVID-19 patients with abnormal GI symptoms.

THE ASEAN JOURNAL OF RADIOLOGY
ISSN 2672-9393

Colonic, rectal abnormalities (29% vs 12%, p=0.3) and small bowel thickening (7% vs 6%, p=0.3) were mostly detected in patients with worse outcomes but not significantly different in both groups, in concordance with the prior studies [12, 19].

COVID-19 is a disease-related consequence that could be deadly due to acute mesenteric ischemia (AMI), results from systemic inflammation, which results in hypercoagulability [21-23]. We encountered one case of acute bowel ischemia. CT imaging reveals non-enhancement of the bowel wall of sigmoid and a descending colon with a filling defect at the proximal inferior mesenteric artery (IMA) which typically indicates acute mesenteric ischemia (AMI) [24] (Figure 2). However, bowel ischemia and intestinal perforation in our study were rare findings, with 3% and 5% line with recent studies [12, 19].

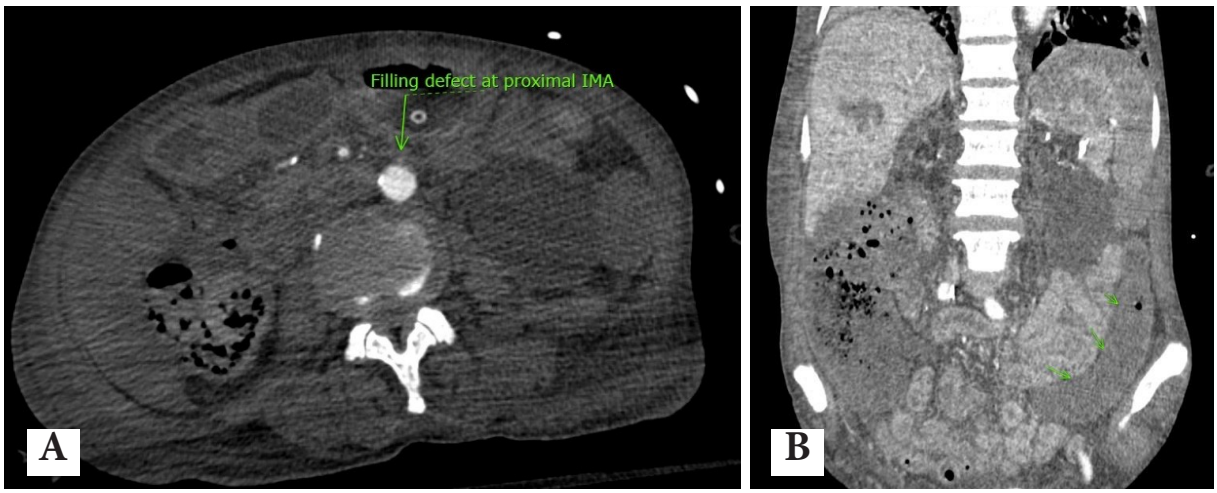

Figure 2. *CT whole abdomen axial view (A) and coronal view (B), a 64-year-old female known case of COVID-19 infection with septic shock, abdominal pain and distension. CT imaging revealed a filling defect at the proximal IMA (A) and non-enhancement of the bowel wall of sigmoid and a descending colon (arrow), which typically indicate acute mesenteric ischemia (AMI) (B).*

A previous study on solid organ infarction showed splenic infarctions in COVID-19, a rare finding in the published literature, as they are frequently accidentally found on contrast-enhanced CT chest (CECT) [25]. In our study, we found about 10% of solid organ infarction. Additional studies are required in order to clarify and correlate with serum biomarkers such as D-dimer levels.

Our study found imaging of hepatitis at 15% which is higher than the previous study [12, 19]. Only a small amount of research has examined the role of abdominal imaging in the assessment and definite imaging features of hepatic involvement in COVID-19, which is still being researched [26]. Further research is needed to establish the significance of COVID-19-related hepatobiliary dysfunction.

The propensity of hypercoagulability in COVID-19 patients increased bleeding manifestations [27]. Regarding the incidence of bleeding in COVID-19 patients, the amount of literature is insufficient, either because of coagulopathy or secondary to anticoagulation treatments [28]. More importantly, the possibility of bleeding complications is increased in anticoagulant treatments with hypercoagulable patients [29]. The majority of studies have reported that the most common bleeding manifestation in seriously ill COVID-19 patients was abdominal hematomas, of which the retroperitoneal compartment was the most common site of bleeding [30-33]. In line with our research, we found all bleeding manifestations up to 27% of which intra-abdominal bleeding was the most common finding (19%) followed by retroperitoneal bleeding (10%) and abdominal wall hematoma (7%). Anticoagulants for venous thromboembolism (VTE) prevention and treatment significantly increased the incidence of all bleeding manifestations (P=0.025) and retroperitoneal bleeding (P=0.034), but did not significantly increase the incidence of intra-abdominal bleeding or abdominal wall hematoma. However, all bleeding manifestations were not significantly associated with worse clinical outcomes. We showed a case of COVID-19 infection on enoxaparin for VTE treatment and developed active bleeding at the left iliacus and left iliopsoas muscles with a large retroperitoneal hematoma. Angiography showed contrast extravasation along the territory of the left L3, L4 lumbar artery and left iliolumbar artery. He underwent gelfoam embolization (Figure 3).

THE ASEAN JOURNAL OF RADIOLOGY
ISSN 2672-9393

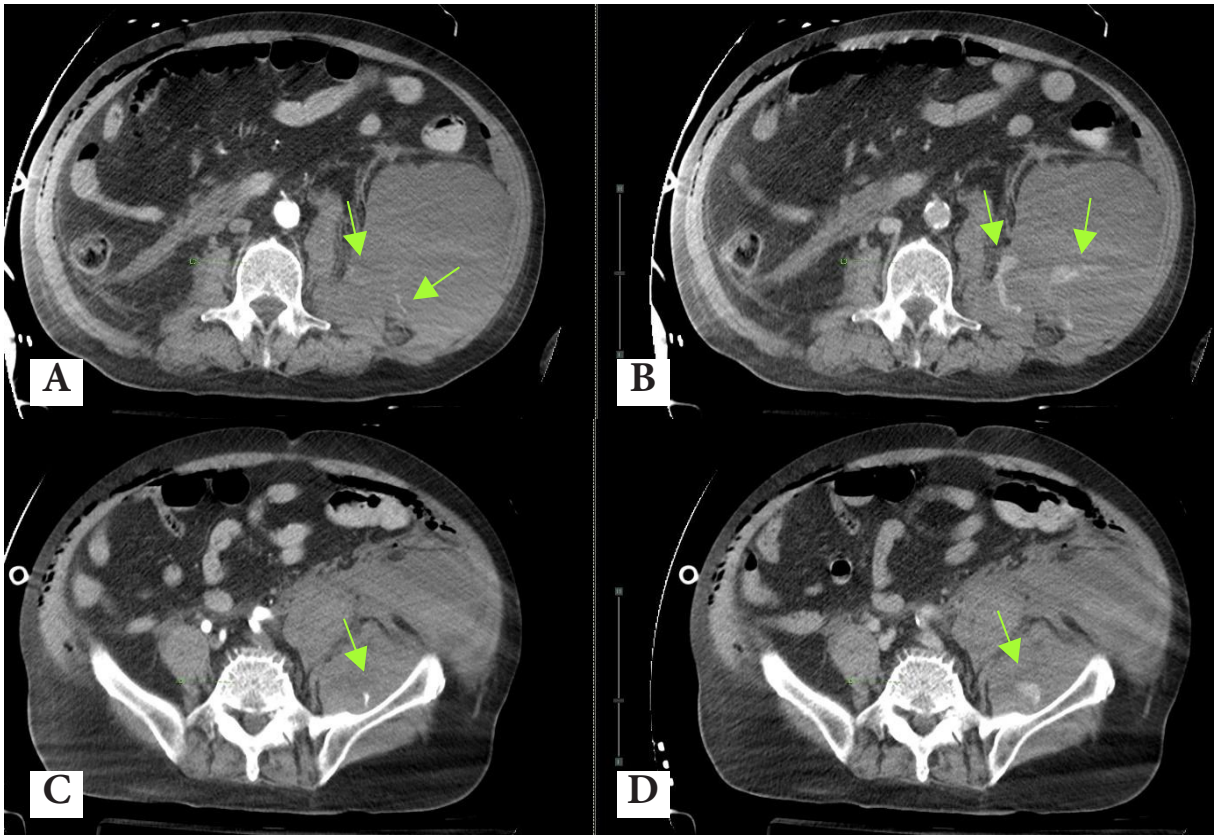

Figure 3. *CT whole abdomen axial view arterial phase (A, C) and portovenous phase (B, D), a 68-year-old male, a known case of COVID-19 infection, given Enoxaparin thromboembolic treatment and developed active bleeding at left iliacus, left iliopsoas muscle (A, B) with large retroperitoneal hematoma (C, D). Angiography showed contrast extravasation along the territory of the left L3 and L4 lumbar arteries, and the left iliolumbar artery (arrow). He underwent gelfoam embolization.*

We also reported patients with abnormal bowel findings would have a higher risk of worse outcomes, invasive mechanical ventilation and death, similar to the result of the previous study [12], but there were no significant statistical correlations. Abnormal bowel findings also indicate higher days of hospitalization but also no significant statistical correlations.

Furthermore, in regard to upcoming research, we believe that multi-center collaborations would produce higher numbers of patient registrations than single-center studies, resulting in a greater data pool and a shorter time to explore topics of concern. Results seem to be statistically significant and represent the entire population.

The limitations of this study included a retrospective study design and a small sample size. Also, there was no inter-reader agreement evaluation and determining imaging findings by consensus. Radiologic-pathologic correlations were not established, and clinical follow-up was not available. Our findings are unable to determine which reported findings are strongly associated with COVID-19. Prospective research with larger samples is needed.

Conclusion

In conclusion, abdominal CT scans performed on COVID-19 patients frequently revealed abnormal bowel findings, which were strongly associated with worse prognosis. Clinicians and surgeons must be concerned about the disease's abdominal signs and symptoms. Finally, radiologists need to be concerned about the abnormal bowel findings and point them out to clinicians and surgeons.

References

1. Huang C, Wang Y, Li X, Ren L, Zhao J, Hu Y, et al. Clinical features of patients infected with 2019 novel coronavirus in Wuhan, China. lancet 2020;395:497-506. doi: 10.1016/S0140-6736(20)30183-5.

2. Guan WJ, Ni ZY, Hu Y, Liang WH, Ou CQ, He JX, et al. Clinical characteristics of coronavirus disease 2019 in China. N Engl J Med 2020;382:1708-20. doi: 10.1056/NEJMoa2002032.

3. Johns Hopkins coronavirus resource center [Internet]. Baltimore (MD) :Johns Hopkins University & Medicine; c2024 [cited 2024 Jun 8]. Available from: https://coronavirus.jhu.edu/about .

4. Cheung KS, Hung IFN, Chan PPY, Lung K, Tso E, Liu R, et al. Gastrointestinal manifestations of SARS-CoV-2 infection and virus load in fecal samples from a Hong Kong cohort: systematic review and meta-analysis. Gastroenterology 2020;159:81-95. doi: 10.1053/j.gastro.2020.03.065.

5. Luo S, Zhang X, Xu H. Don't overlook digestive symptoms in patients with 2019 novel coronavirus disease (COVID-19). Clin Gastroenterol Hepatol 2020;18:1636-7. doi: 10.1016/j.cgh.2020.03.043.

6. Pan L, Mu M, Yang P, Sun Y, Wang R, Yan J, et al. Clinical characteristics of COVID-19 patients with digestive symptoms in Hubei, China: a descriptive, cross-sectional, multicenter study. Am J Gastroenterol 2020;115:766-73. doi: 10.14309/ajg.0000000000000620.

7. Gu J, Han B, Wang J. COVID-19: gastrointestinal manifestations and potential fecal–oral transmission. Gastroenterology 2020;158:1518-9. doi: 10.1053/j.gastro.2020.02.054.

8. Hoffmann M, Kleine-Weber H, Schroeder S, Krüger N, Herrler T, Erichsen S, et al. SARS-CoV-2 cell entry depends on ACE2 and TMPRSS2 and is blocked by a clinically proven protease inhibitor. Cell 2020;181:271-80.e8. doi: 10.1016/j.cell.2020.02.052.

9. Hamming I, Timens W, Bulthuis ML, Lely AT, Navis G, van Goor H. Tissue distribution of ACE2 protein, the functional receptor for SARS coronavirus. A first step in understanding SARS pathogenesis. J Pathol 2004;203:631-7. doi: 10.1002/path.1570.

10. Harmer D, Gilbert M, Borman R, Clark KL. Quantitative mRNA expression profiling of ACE 2, a novel homologue of angiotensin converting enzyme. FEBS lett 2002;532:107-10. doi: 10.1016/s0014-5793(02)03640-2.

11. Mao R, Liang J, Shen J, Ghosh S, Zhu LR, Yang H, et al. Implications of COVID-19 for patients with pre-existing digestive diseases. Lancet Gastroenterol Hepatol 2020;5:425-7. doi: 10.1016/S2468-1253(20)30076-5.

12. Bhayana R, Som A, Li MD, Carey DE, Anderson MA, Blake MA, et al. Abdominal imaging findings in COVID-19: preliminary observations. Radiology 2020;297:E207. doi: 10.1148/radiol.2020201908.

13. Gornet JM, Tran Minh MT, Leleu F, Hassid D. What do surgeons need to know about the digestive disorders and paraclinical abnormalities induced by COVID-19? J Visc Surg 2020;157(3 Suppl 1):S51-7. doi: 10.1016/j.jviscsurg.2020.04.017.

14. A Beccara L, Pacioni C, Ponton S, Francavilla S, Cuzzoli A. Arterial mesenteric thrombosis as a complication of SARS-CoV-2 infection. Eur J Case Rep Intern Med 2020;7:001690. doi: 10.12890/2020_001690.

15. Guo Y, Hu X, Yu F, Chen J, Zheng W, Liu J, et al. Abdomen CT findings in a COVID-19 patient with intestinal symptoms and possibly false negative RT-PCR before initial discharge. Quant Imaging Med Surg 2020;10:1158-61. doi: 10.21037/qims-20-463.

16. de Barry O, Mekki A, Diffre C, Seror M, El Hajjam M, Carlier RY. Arterial and venous abdominal thrombosis in a 79-year-old woman with COVID-19 pneumonia. Radiol Case Rep 2020;15:1054-7. doi: 10.1016/j.radcr.2020.04.055.

17. Zhou F, Yu T, Du R, Fan G, Liu Y, Liu Z, et al. Clinical course and risk factors for mortality of adult inpatients with COVID-19 in Wuhan, China: a retrospective cohort study. Lancet 2020;395:1054-62. doi: 10.1016/S0140-6736(20)30566-3.

18. Crawford SE, Ramani S, Blutt SE, Estes MK. Organoids to dissect gastrointestinal virus–hostiInteractions: What have we learned? Viruses 2021; 13:999. doi: 10.3390/v13060999.

19. Horvat N, Pinto PVA, Araujo-Filho JAB, Santos JMMM, Dias AB, Miranda JA, et al. Abdominal gastrointestinal imaging findings on computed tomography in patients with COVID-19 and correlation with clinical outcomes. Eur J Radiol Open 2021;8:100326. doi: 10.1016/j.ejro.2021.100326..

20. Goldberg-Stein S, Fink A, Paroder V, Kobi M, Yee J, Chernyak V. Abdominopelvic CT findings in patients with novel coronavirus disease 2019 (COVID-19). Abdom Radiol (NY) 2020;45:2613-23. doi: 10.1007/s00261-020-02669-2.

21. Parry AH, Wani AH, Yaseen M. Acute mesenteric ischemia in severe coronavirus-19 (COVID-19): possible mechanisms and diagnostic pathway. Acad Radiol 2020;27:1190. doi: 10.1016/j.acra.2020.05.016.

22. Lodigiani C, Iapichino G, Carenzo L, Cecconi M, Ferrazzi P, Sebastian T, et al. Venous and arterial thromboembolic complications in COVID-19 patients admitted to an academic hospital in Milan, Italy. Thromb Res 2020;191:9-14. doi: 10.1016/j.thromres.2020.04.024.

23. Escher R, Breakey N, Lämmle B. Severe COVID-19 infection associated with endothelial activation. Thromb Res 2020;190:62. doi: 10.1016/j.thromres. 2020.04.014.

24. Varga Z, Flammer AJ, Steiger P, Haberecker M, Andermatt R, Zinkernagel AS, et al. Endothelial cell infection and endotheliitis in COVID-19. Lancet 2020;395:1417-8. doi: 10.1016/S0140-6736(20)30937-5.

25. Santos Leite Pessoa M, Franco Costa Lima C, Farias Pimentel AC, Godeiro Costa JC, Bezerra Holanda JL. Multisystemic infarctions in COVID-19: focus on the spleen. Eur J Case Rep Intern Med 2020;7:001747. doi: 10.12890/2020_001747.

26. Vaidya T, Nanivadekar A, Patel R. Imaging spectrum of abdominal manifestations of COVID-19. World J Radiol 2021 ;13:157-70. doi: 10.4329/wjr.v13.i6.157.

27. Klok FA, Kruip MJHA, van der Meer NJM, Arbous MS, Gommers DAMPJ, Kant KM, et al. Incidence of thrombotic complications in critically ill ICU patients with COVID-19. Thromb Res 2020;191:145-7. doi: 10.1016/j.thromres.2020.04.013.

28. Tang N, Li D, Wang X, Sun Z. Abnormal coagulation parameters are associated with poor prognosis in patients with novel coronavirus pneumonia. J Thromb Haemost 2020;18:844-7. doi: 10.1111/jth.14768.

29. Al-Samkari H, Karp Leaf RS, Dzik WH, Carlson JCT, Fogerty AE, Waheed A, et al. COVID-19 and coagulation: bleeding and thrombotic manifestations of SARS-CoV-2 infection. Blood 2020;136:489-500. doi: 10.1182/blood.2020006520.

30. Mazzitelli M, Serapide F, Tassone B, Laganà D, Trecarichi EM, Torti C. Spontaneous and severe haematomas in patients with COVID-19 on low-molecular-weight heparin for paroxysmal atrial fibrillation. J Hematol Infect Dis 2020 ;12:e2020054. doi: 10.4084/MJHID.2020.054.

31. Scialpi M, Russo P, Piane E, Gallo E, Scalera GB. First case of retroperitoneal hematoma in COVID-19. Turk J Urol 2020;46:407-9. doi: 10.5152/tud.2020.20302.

THE ASEAN JOURNAL OF RADIOLOGY
ISSN 2672-9393

32. Zhang J, He X, Hu J, Li T. Retroperitoneal hemorrhage during veno-venous extracorporeal membrane oxygenation in COVID-19 patientss: clinical experience and review of literature. Research Square [Internet]. 2024 [cited 2024 Jun 7]. Available from: https://www.researchsquare.com/article/rs-32685/v1

33. Erdinc B, Raina JS. Spontaneous retroperitoneal bleed coincided with massive acute deep vein thrombosis as initial presentation of COVID-19. Cureus 2020;12:e9772. doi: 10.7759/cureus.9772.

Original Article

Comparison between the use of one and two CT scans for attenuation correction of rest-stress myocardial perfusion SPECT with Tc-99m sestamibi

Taratip Narawong, M.Sc.[(1)]
Kanyalak Wiyaporn, Ph.D.[(2)]
From [(1)] Division of Nuclear Medicine, Department of Radiology, Rajavithi Hospital, Bangkok, Thailand.
[(2)] Department of Radiological Technology, Faculty of Medical Technology, Mahidol University, Bangkok, Thailand.
Address correspondence to K.W. (email: kanyalak.wiy@mahidol.ac.th, kanyalak.wiy@mahidol.edu)

Received 22 January 2024; revised 5 April 2024; accepted 2 May 2024
doi:10.46475/asean-jr.v25i2.895

Abstract

Background: The standard protocol is to use separate computed tomography (CT) scans acquired during rest and stress for attenuation correction (AC) of myocardial perfusion (MP) single photon emission computed tomography (SPECT) imaging. Recently, there have been attempts to reduce the radiation dose by using one CT instead of two CTs.

Objective: To compare between the use of one and two CTs for AC of rest-stress MP SPECT with Tc-99m sestamibi in quantification of MP and left ventricle (LV) function.

THE ASEAN JOURNAL OF RADIOLOGY
ISSN 2672-9393

Materials and methods: Gated rest-stress MP SPECT images of 107 patients were reprocessed using 3 different AC methods: 1) rest CT for AC of rest SPECT and stress CT for AC of stress SPECT (2CT); 2) rest CT for AC of both rest and stress SPECT (1CT-rest); and 3) stress CT for AC of both rest and stress SPECT (1CT-stress). SPECT images obtained from 2CT and 1CT were used for quantification of MP values and LV function values. The values from 2CT and 1CT were compared.

Results: The MP values of 2CT and 1CT showed a strong correlation ($r \geq 0.712$) and they did not differ significantly ($p=0.106$ to 0.931). In contrast, the LV function values of 2CT and 1CT exhibited a very strong correlation ($r \geq 0.960$), but they differ significantly ($p=<0.001$ to 0.004).

Conclusion: The use of one and two CTs for AC in rest-stress MP SPECT with Tc-99m sestamibi can be interchanged for the quantification of MP, but not for the quantification of LV function.

Keywords: CT-based attenuation correction, Gated SPECT, Left ventricle function, Myocardial perfusion SPECT, Tc-99m sestamibi.

Introduction

Myocardial perfusion single photon emission computed tomography (MP SPECT) imaging has for several decades been one of the most widely used examinations in the diagnosis, risk stratification, and evaluation of treatment efficacy in patients with a suspected or known coronary artery disease (CAD) [1-6]. This perfusion imaging uses an intravenously administered radiopharmaceutical, such as technetium-99m (Tc-99m) sestamibi, to depict the distribution of blood flow in the myocardium. Myocardial perfusion SPECT imaging at rest and during cardiovascular stress allows differentiation between myocardial ischemia (limitations in blood flow) and infarction (absence of blood flow) [7, 8]. In addition to regional perfusion, acquiring MP SPECT data with electrocardiographic (ECG) gating (gated MP SPECT), allows measurement of cardiac function index such as left

ventricle volume, ejection fraction (EF), and regional wall motion and thickening. Gated MP SPECT, with the ability to evaluate both myocardial perfusion and cardiac function, has become a routine protocol, and it expands the clinical utility of myocardial perfusion SPECT [7, 9-13].

Although gated MP SPECT is a valuable diagnostic tool, soft-tissue attenuation in the abdomen, breasts, diaphragm, and lateral chest wall causes attenuation artifacts, with an attendant decrease in the interpretive confidence of the reader and the diagnostic accuracy of the examination [14-16]. Computed tomography-based attenuation correction (CTAC) is a methodology that applies an attenuation map derived from computed tomography (CT) to SPECT in order to compensate for this degradation. Attenuation correction (AC) produces qualitative and quantitative data that can more accurately represent relative myocardial per¬fusion and improve the performance of myocardial perfusion SPECT interpreta-tion, especially the specificity of myocardial ischemia [7, 17-20].

Common gated rest-stress MP SPECT requires two scans taken at rest and after exercise or pharmacologic stress. For accurate CTAC, it is standard to acquire separate CT scans during rest and stress, causing additional radiation exposure to the patient. Recently, there have been attempts to reduce the radiation dose from MP SPECT while maintaining diagnostic accuracy [21, 22], and it has been proposed that one CT may be sufficient for AC of both rest and stress SPECT to reproduce accurate quantification of myocardial perfusion. The effectiveness of using one CT for this purpose has been evaluated previously [23-26]; however, few studies have been performed of the efficacy of using one CT for AC of gated rest-stress MP SPECT in quantification of the left ventricle (LV) function.

The aim of this study was to compare the use of one and two CTs for AC of gated rest-stress MP SPECT imaging with Tc-99m sestamibi in quantification of myocardial perfusion and LV function.

THE ASEAN JOURNAL OF RADIOLOGY
ISSN 2672-9393

Materials and methods

Study population

This study retrospectively analyzed the data of 107 patients who underwent gated rest-stress MP SPECT/CT imaging with Tc-99m sestamibi between March 2020 and December 2021. The image data from patients who were unable to complete gated rest-stress myocardial perfusion (MP) SPECT/CT imaging, including rest SPECT, rest CT, stress SPECT, and stress CT scans, as well as patients with a significant liver, gall bladder, and bowel activity, which led to interference in myocardial uptake as observed in SPECT images, were excluded from this study. Table 1 shows the demographics of the study population. The proportion of male and female patients was approximately equal. This study was approved by the research ethics committee of Rajavithi Hospital (#221/2564).

Table 1. *Demographics of the study population (n = 107).*

Patient characteristics	Forum program
Male sex	52 (48.6%)
Age (years)	63 ± 12
Body-mass index (m^2/kg)	25.8 ± 5.4
Abnormal MP SPECT (ischemia or infarction)[a]	38 (35.51%)

Data are mean ± standard deviation (SD) or number, with percentages in parentheses.
[a]The interpretation results reported by nuclear medicine radiologists.

Gated MP SPECT data acquisition

All 107 patients were imaged with the dual-headed detector SPECT system, NM/CT 870 DR (GE Healthcare), using a standard one-day rest/stress imaging protocol with CT acquired for AC both at rest and during stress. Firstly, SPECT and CT data were acquired at rest (rest SPECT and rest CT) and the data were acquired 3 hours later. The imaging protocol of one-day rest/stress MP SPECT/CT is shown in Figure 1.

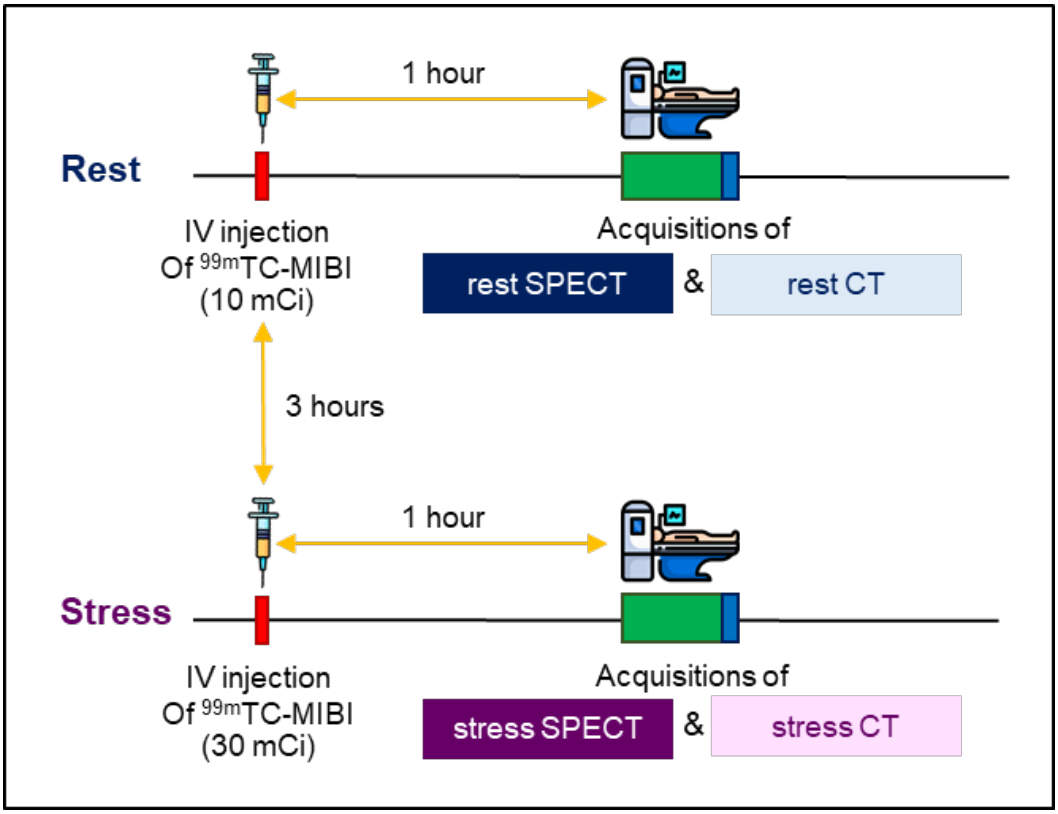

Figure 1. *Imaging protocol of one-day rest/stress MP SPECT/CT.*

At rest, patients were intravenously injected with 10 mCi of Tc-99m sestamibi, and gated MP SPECT imaging was performed 1 hour after injection. Two SPECT detectors coupled with low energy high resolution sensitivity (LEHRS) parallel-hole collimators were positioned at 90° to each other (L mode) and were rotated 180° from the right anterior oblique (RAO) 45° to the left posterior oblique (LPO) 45° with a view angle of 3°. Matrix sizes were set at 64 × 64 with the zoom factor of 1.5 and data were acquired for 20 seconds at each view. The energy windows were set at 140 keV ± 10% for the main window and 120 keV ± 5% for the scatter window. The gated data were acquired with 8 frames per R-R intervals. CT acquisition for AC was performed immediately after the SPECT acquisition with free breathing. The CT data was acquired at 120 kV, 20 mA and a slice thickness of 5 mm.

THE ASEAN JOURNAL OF RADIOLOGY
ISSN 2672-9393

Stress tests were started at 3 hours after injection of Tc-99m sestamibi with patients in a resting condition. Pharmacological stress with adenosine was used in 90% of the patients and exercise stress was used for the remainder. The 30 mCi dose (3 times greater than the rest activity) of Tc-99m sestamibi was intravenously injected into the patients under the stress condition. The stress SPECT data was acquired before CT acquisition. The patient positioning and acquisition protocols of stress SPECT and CT were similar to those of the rest protocols, except for the time per view of SPECT acquisition. The time per view of SPECT acquisition for stress SPECT (15 seconds) was shorter than that of rest SPECT (20 seconds) in order to minimize the effects of cardiac and respiratory motions on the MP SPECT images during stress. All patients were scanned in a supine position with feet first, arms raised on the armrest, both at rest and under stress, to maintain the same positioning between acquisitions.

Image reconstruction & Quantitative analysis

The SPECT data (gated and non-gated) and CT data for both rest and stress (rest SPECT, rest CT, stress SPECT and stress CT) were used for SPECT image reconstruction with CTAC and quantitative analysis. The rest and stress SPECT images were reconstructed using ordered subset-expectation maximization (OS-EM) with 2 iterations and 10 subsets on a Xeleris workstation (GE Healthcare). Left ventricular activity was masked from liver, gall bladder and bowel activities. Scatter correction was based on the subtraction of projection data, with no method for motion correction. Butterworth filter was applied to reconstruct images with cut-off frequency of 0.45 and 0.548 cycles/cm and order of 10 and 12.6 for rest SPECT and stress SPECT, respectively.

CTAC was performed during SPECT image reconstruction. A single radiological technologist with expertise in gated MP SPECT analysis (> 20 years of experience) processed all gated MP SPECT studies with different CTAC methods (Figure 2) in order to investigate this research aim. The standard CTAC method was to use rest CT for AC of rest SPECT and stress CT for AC of stress SPECT, noted as 2CT (Figure 2a). The alternative method was to use rest CT for AC of both rest and stress SPECT, noted as 1CT-rest (Figure 2b). Another alternative method

was to use stress CT for AC of both rest and stress SPECT noted as 1CT-stress (Figure 2c). The software for image reconstruction automatically performed image registration between SPECT and CT images for CTAC, and the alignment of the SPECT and CT images was visually confirmed and adjusted in the axial, sagittal, and coronal planes for every patient.

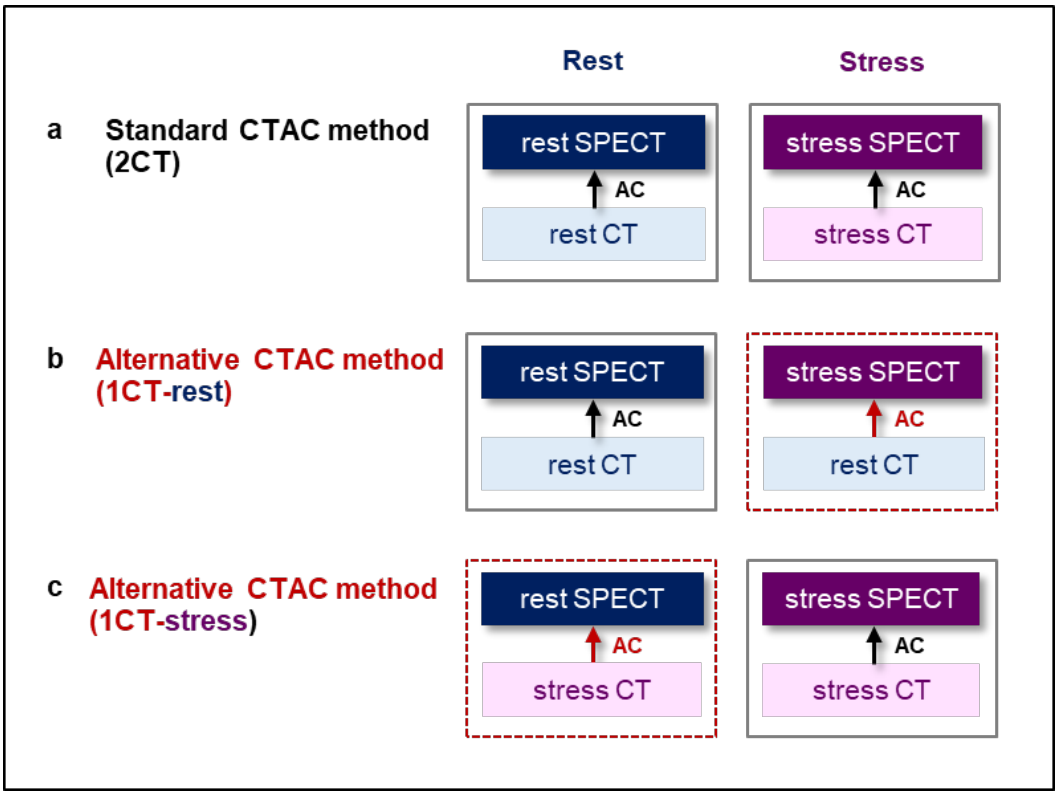

Figure 2. *SPECT image reconstruction with different CTAC methods: (a) standard CTAC method (2CT): using rest CT for AC of rest SPECT and stress CT for AC of stress SPECT; (b) alternative CTAC method (1CT-rest): using rest CT for AC of both rest and stress SPECT; and (c) alternative CTAC method (1CT-stress): using stress CT for AC of both rest and stress SPECT.*

THE ASEAN JOURNAL OF RADIOLOGY
ISSN 2672-9393

We used Quantitative Perfusion SPECT (QPS) and Myometrix software for the quantitative analysis of gated MP SPECT imaging because these methods are routinely used in our hospital. The reconstructed MP SPECT images with different CTAC methods from non-gated data were used for quantification of myocardial perfusion values, including summed rest score (SRS), summed stress score (SSS) summed difference score (SDS), rest total perfusion deficit (rest TPD), stress total perfusion deficit (stress TPD) and transient ischemic dilation ratio (TID) [8, 27]. The MP SPECT images were automatically compared with a normalized database with QPS software to produce sum scores according to anatomic regions on a 17-segment American Heart Association polar map. The SRS and SSS were calculated as the sum of the individual scores from the 17 segments of the polar map obtained during rest and stress. The SDS was calculated by subtracting the SRS from the SSS (SDS = SSS-SRS). These values indicate the severity of myocardial ischemia. TPD was calculated based on both the extent and severity of ischemia. The TID, which is the ratio of the stress LV volume to rest LV volume, was quantified using Myometrix software; this value is one of the markers of severe myocardial ischemia.

The reconstructed MP SPECT images obtained from different CTAC methods from gated data were used for quantification of LV function values, including rest end diastolic volume (EDV), stress EDV, rest end systolic volume (ESV), stress ESV, rest ejection fraction (EF), and stress EF using Myometrix software. The percentage of EF was calculated as follows: EDV-ESV/EDV*100 [13]. The EF is clinically used as an index for evaluation of the cardiac function.

Statistical analysis

All quantitative values were represented as mean ± standard deviation (SD). Pearson's correlation was used to test the correlation between quantitative values obtained from 2CT and 1CT. An arbitrary classification for Pearson's correlation was: ≥0.800, very strong; 0.600-0.799, strong; 0.400-0.599, moderate; 0.200-0.399, weak; and <0.200, very weak. The quantitative values between 2CT and 1CT were compared using paired t-test, and $p < 0.05$ was considered statistically significant.

Results

Table 2 summarizes the findings, with mean ± SD of all quantitative values, and the correlation and the comparison of quantitative values of 2CT and 1CT. There was a very strong correlation between myocardial perfusion values obtained from 2CT and 1CT for SRS of 2CT and 1CT-stress, SSS of 2CT and 1CT-rest, SDS of 2CT and 1CT-stress, Rest TPD of 2CT and 1CT-stress, Stress TPD of 2CT and 1CT-rest, TID of 2CT and 1CT-stress, and TID of the 2CT and 1CT-rest ($r \geq 0.915$), as shown in Table 2. The correlation coefficient of SDS between 2CT and 1CT-rest ($r = 0.712$), which indicated a strong correlation, was lower than that of other myocardial perfusion values. This corresponded to the 3D scatter plots in Figure 3 in which the variability in the SDS from 2CT and 1CT-rest was seen to be the highest (Figure 3d) among other myocardial perfusion values (Figure 3a, 3b, 3c, 3e, 3f, 3g and 3h). However, the comparison results showed that there was no significant difference between myocardial perfusion values from 2CT and 1CT, as shown in the last column of Table 2.

THE ASEAN JOURNAL OF RADIOLOGY
ISSN 2672-9393

Table 2. *Correlation and comparison of quantitative values obtained from 2CT and 1CT.*

Quantitative Values (2CT vs. 1CT)	Mean ± Standard Deviation (2CT vs. 1CT)	Correlation Coefficient (r)	Difference (p value)
Myocardial Perfusion Values			
SRS_{2CT} vs. $SRS_{1CT\text{-}stress}$	3.7 ± 8.3 vs. 3.7 ± 8.4	0.991[a]	0.931
SSS_{2CT} vs. $SSS_{1CT\text{-}rest}$	6.9 ± 9.1 vs. 7.0 ± 9.2	0.974[a]	0.647
SDS_{2CT} vs. $SDS_{1CT\text{-}stress}$	3.1 ± 2.6 vs. 3.1 ± 2.8	0.920[a]	0.931
SDS_{2CT} vs. $SDS_{1CT\text{-}rest}$	3.1 ± 2.6 vs. 3.2 ± 2.9	0.712[b]	0.647
Rest TPD_{2CT} vs. Rest $TPD_{1CT\text{-}stress}$	6.2 ± 9.5 vs. 6.2 ± 9.1	0.980[a]	0.918
Stress TPD_{2CT} vs. Stress $TPD_{1CT\text{-}rest}$	7.7 ± 9.6 vs. 7.7 ± 9.7	0.986[a]	0.680
TID_{2CT} vs. $TID_{1CT\text{-}stress}$	1.1 ± 0.1 vs. 1.1 ± 0.1	0.915[a]	0.571
TID_{2CT} vs. $TID_{1CT\text{-}rest}$	1.1 ± 0.1 vs. 1.1 ± 0.1	0.924[a]	0.106
LV Function Values			
Rest EDV_{2CT} vs. Rest $EDV_{1CT\text{-}stress}$ (mL)	82.7 ± 52.2 vs. 89.4 ± 50.1	0.982[a]	<0.001*
Stress EDV_{2CT} vs. Stress $EDV_{1CT\text{-}rest}$ (mL)	89.1 ± 54.4 vs. 92.9 ± 54.5	0.987[a]	<0.001*
Rest ESV_{2CT} vs. Rest $ESV_{1CT\text{-}stress}$ (mL)	41.6 ± 46.6 vs. 45.3 ± 47.1	0.973[a]	0.001*
Stress ESV_{2CT} vs. Stress $ESV_{1CT\text{-}rest}$ (mL)	45.7 ± 48.0 vs. 48.7 ± 49.9	0.979[a]	0.023*
Rest EF_{2CT} vs. Rest $EF_{1CT\text{-}stress}$ (%)	58.7 ± 17.7 vs. 57.7 ± 17.8	0.960[a]	0.031*
Stress EF_{2CT} vs. Stress $EF_{1CT\text{-}rest}$ (%)	57.0 ± 16.9 vs. 6.1 ± 17.4	0.983[a]	0.004*

Pearson's correlation was used to determine the correlation between quantitative values from 2CT and 1CT.
[a]very strong correlation (r in the range of 0.800-1.000); [b]strong correlation (r in the range of 0.600-0.799).
Paired t-test was used to determine the significance of the differences (p values) between quantitative values from the 2CT and 1CT.
**significant difference (p<0.05).*

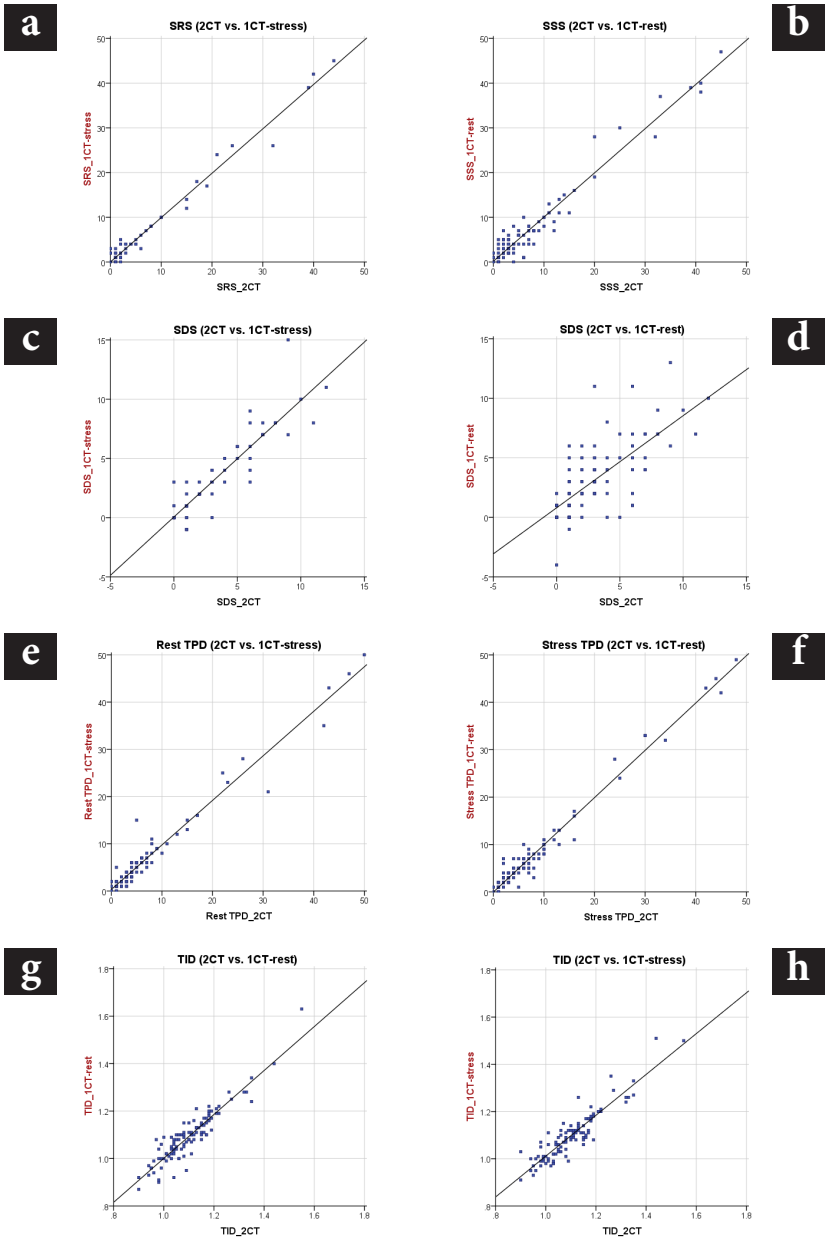

Figure 3. *Correlation between myocardial perfusion values from 2CT and 1CT: (a) SRS_{2CT} vs. $SRS_{1CT\text{-}stress}$; (b) SSS_{2CT} vs. $SSS_{1CT\text{-}rest}$; (c) SDS_{2CT} vs. $SDS_{1CT\text{-}stress}$; (d) SDS_{2CT} vs. $SDS_{1CT\text{-}rest}$; (e) Rest TPD_{2CT} vs. Rest $TPD_{1CT\text{-}stress}$; (f) Stress TPD_{2CT} vs. Stress $TPD_{1CT\text{-}rest}$; (g) TID_{2CT} vs. $TID_{1CT\text{-}stress}$; and (h) TID_{2CT} vs. $TID_{1CT\text{-}rest}$.*

THE ASEAN JOURNAL OF RADIOLOGY
ISSN 2672-9393

The SDS was of interest in this study because it can be clinically used as an index for diagnosis of myocardial ischemia. The SDS was 3.1 ± 2.6 for 2CT and 3.1 ± 2.8 for 1CT-stress, and these values were not significantly different (p = 0.931). The SDS of 1CT-rest was 3.2 ± 2.9 and did not significantly differ from that of 2CT (p = 0.647). Figure 4 and 5 shows a comparison of 2CT and 1CT when the SDS values were classified into four groups: no ischemia (SDS 0-1); mild ischemia (SDS 2-4); moderate ischemia (SDS 5-6); and severe ischemia (SDS ≥ 7). There was concordance between diagnoses using SDS in 2CT and 1CT-stress in 91.7%, 91.3%, 58.3% and 100.0% of patients with no ischemia, mild ischemia, moderate ischemia, and severe ischemia respectively (Figure 4a). The overall concordance between diagnosis using SDS in 2CT and 1CT-stress was 88.8% (95 from 107 patients) while the discordance was 11.2% (12 from 107 patients) (Figure 4b). Figure 5a shows the concordance of diagnosis using SDS with 2CT and 1CT-rest: 75.0%, 71.7%, 33.3% and 69.2% in patients with no ischemia, mild ischemia, moderate ischemia, and severe ischemia respectively. The overall concordance of diagnosis using SDS with 2CT and 1CT-rest was 68.2% (73 from 107 patients) while the discordance was 31.8% (34 from 107 patients) (Figure 5b).

a

SDS		1CT-stress				Concordance (%)
		No Ischemia	Mild Ischemia	Moderate Ischemia	Severe Ischemia	
2CT	No Ischemia	33	3	0	0	91.7
	Mild Ischemia	1	42	3	0	91.3
	Moderate Ischemia	0	3	7	2	58.3
	Severe Ischemia	0	0	0	13	100.0

b

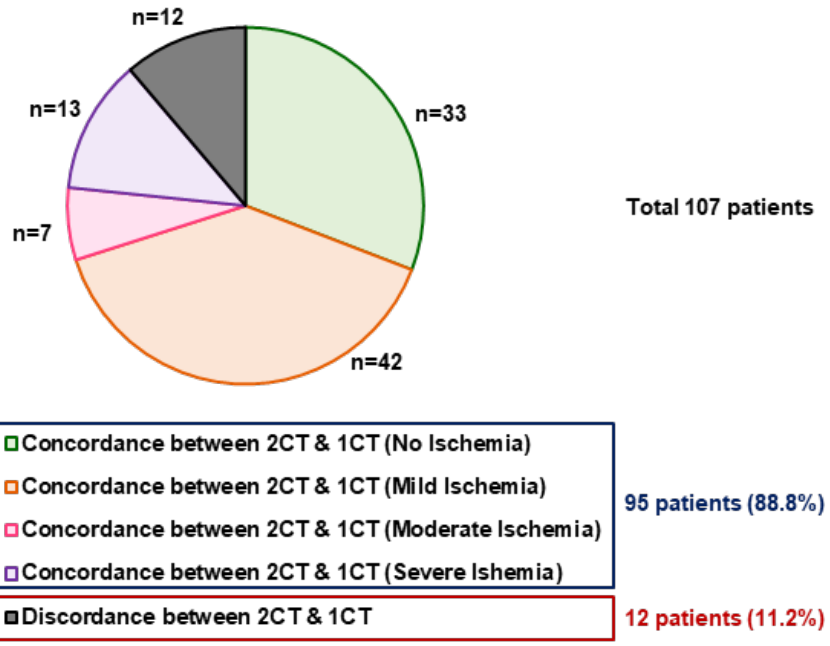

Figure 4. *(a) Concordance between 2CT and 1CT-stress for classification of SDS defined as no ischemia (0-1), mild ischemia (2-4), moderate ischemia (5-6), and severe ischemia (≥ 7) and (b) pie chart showing numbers of patients with concordance in each classification and discordance between 2CT and 1CT-stress.*

a

SDS		1CT-rest				Concordance (%)
		No Ischemia	Mild Ischemia	Moderate Ischemia	Severe Ischemia	
2CT	No Ischemia	27	7	2	0	75.0
	Mild Ischemia	3	33	8	2	71.7
	Moderate Ischemia	3	2	4	3	33.3
	Severe Ischemia	0	2	2	9	69.2

b

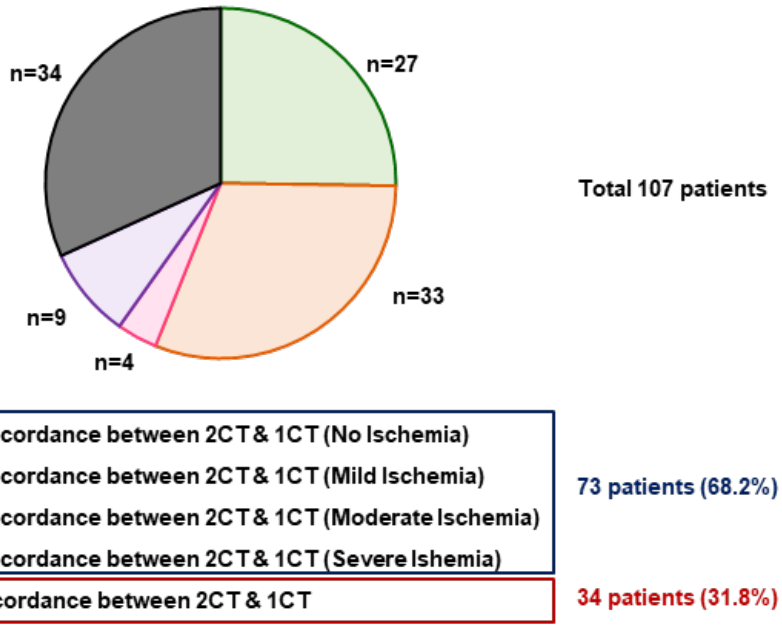

Figure 5. *(a) Concordance between 2CT and 1CT-rest for classification of SDS defined as no ischemia (0-1), mild ischemia (2-4), moderate ischemia (5-6), and severe ischemia (≥ 7) and (b) pie chart showing the number of patients with concordance in each classification and discordance between 2CT and 1CT-rest.*

Figure 6 depicts the correlation between LV function values in 2CT and 1CT. There was a very strong correlation between 2CT and 1CT for all LV function values ($r \geq 0.960$) (Table 2). However, there were significant differences between values for rest EDV, rest ESV, stress EDV, stress ESV, rest EF and stress EF in 2CT and 1CT, as shown in the last column of Table 2.

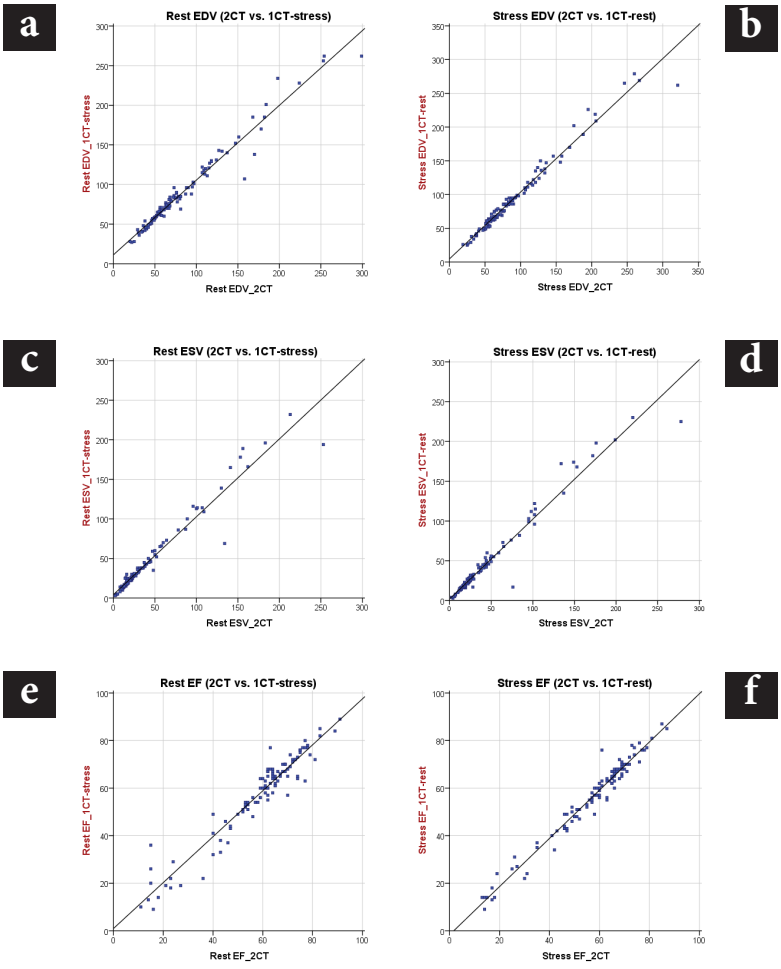

Figure 6. *Correlation between LV function values in 2CT and 1CT: (a) Rest EDV_{2CT} vs. Rest $EDV_{1CT\text{-}stress}$; (b) Stress EDV_{2CT} vs. Stress $EDV_{1CT\text{-}rest}$; (c) Rest ESV_{2CT} vs. Rest $ESV_{1CT\text{-}stress}$; (d) Stress ESV_{2CT} vs. Stress $ESV_{1CT\text{-}rest}$; (e) Rest EF_{2CT} vs. Rest $EF_{1CT\text{-}stress}$; and (f) Stress EF_{2CT} vs. Stress $EF_{1CT\text{-}rest}$.*

THE ASEAN JOURNAL OF RADIOLOGY
ISSN 2672-9393

The EF was considered because it is clinically used as an index for interpretation of the cardiac function. The rest EF values, 58.7 ± 17.7 for 2CT and 57.7 ± 17.8 for 1CT, were significantly different ($p = 0.031$). The stress EF was 57.0 ± 16.9 for 2CT and 56.1 ± 17.4 for 1CT, and these differences were also statistically different ($p = 0.004$). Figures 7 and 8 show a comparison between 2CT and 1CT when the EF levels were categorized into three groups: reduced EF (EF 0-40%); borderline EF (EF 41-49%); and normal EF (EF ≥50%). There was concordance of interpretation using rest EF in 2CT and 1CT-stress in 87.5%, 50.0% and 97.6% of patients for reduced EF, borderline EF, and normal EF, respectively (Figure 7a). The overall concordance of rest EF interpretation was 93.5% (100 from 107 patients) while the discordance was 6.5% (7 from 107 patients) (Figure 7b). The comparison between stress EF in 2CT and 1CT when the EF values were categorized into the same three groups is shown in Figure 8a. There was concordance of interpretation using stress EF in 2CT and 1CT-rest in 100%, 66.7% and 95.0% of patients with reduced EF, borderline EF, and normal EF respectively. The overall concordance of stress EF interpretation was 92.5% (99 from 107 patients) while the discordance was 7.5% (8 from 107 patients) (Figure 8b).

a

Rest EF		1CT-stress			Concordance (%)
		Reduced EF	Borderline EF	Normal EF	
2CT	Reduced EF	14	2	0	87.5
	Borderline EF	3	3	0	50.0
	Normal EF	0	2	83	97.6

b

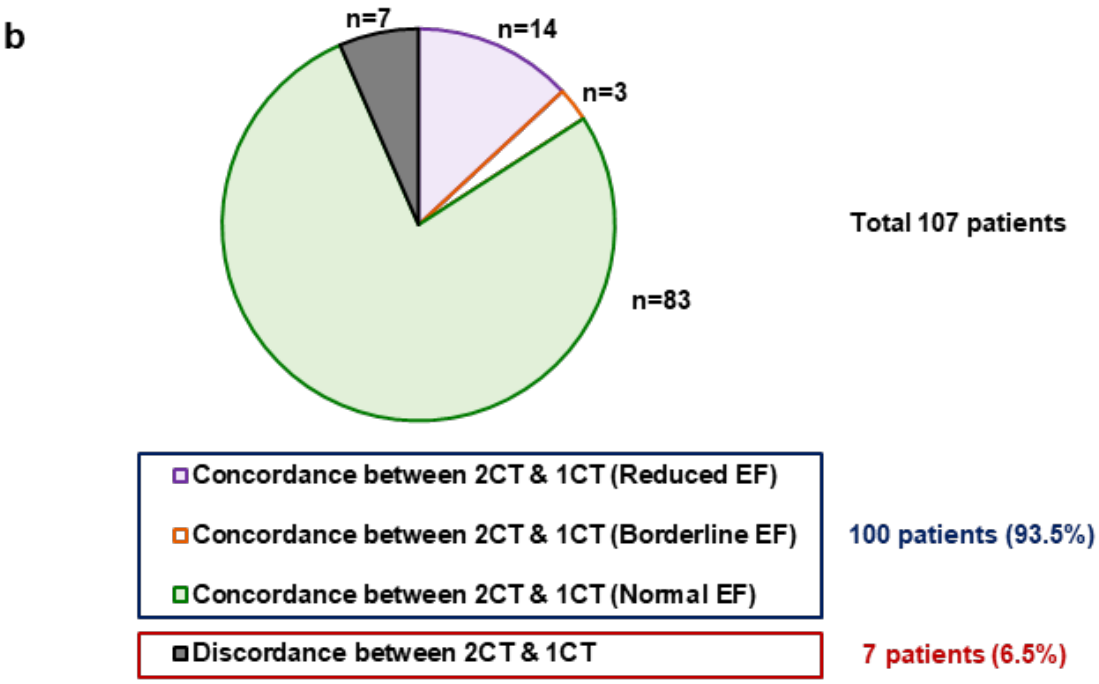

Figure 7. *(a) Concordance between 2CT and 1CT for interpretation of categories of EF defined as reduced rest EF (0-40%), borderline EF (41-49%) and normal EF (≥50%) and (b) pie chart showing the number of patients with concordance in each category and discordance between 2CT and 1CT of rest EF.*

a

Stress EF		1CT-rest			Concordance (%)
		Reduced EF	Borderline EF	Normal EF	
2CT	Reduced EF	145	0	0	100.0
	Borderline EF	2	8	2	66.7
	Normal EF	0	4	76	95.0

b

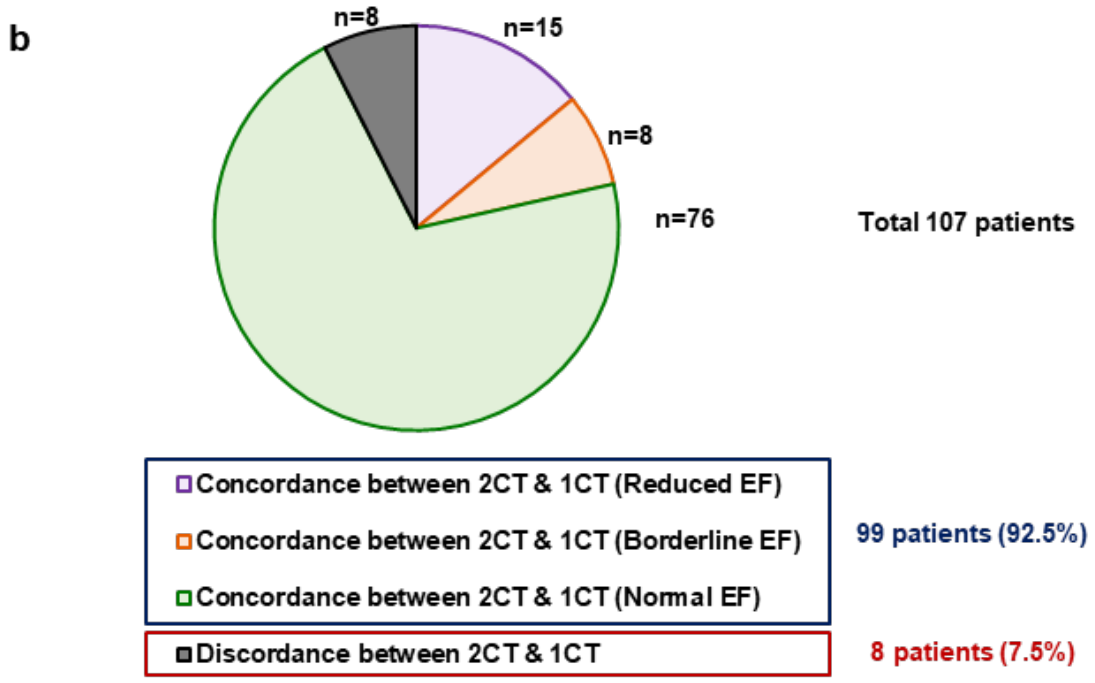

Figure 8. *(a) Concordance between 2CT and 1CT for interpretation of categories of stress EF defined as reduced EF (0-40%), borderline EF (41-49%) and normal EF (≥50%) and (b) pie chart showing the number of patients with concordance in each category and discordance between 2CT and 1CT of stress EF.*

Discussion

Four image acquisitions are required for conventional rest-stress MP SPECT imaging: rest SPECT, rest CT, stress SPECT and stress CT. The standard CTAC method (two CTs) is to use rest CT for AC of rest SPECT and stress CT for AC of stress SPECT. This study aimed to compare the use of two CT scans (2CT) and one CT scan (1CT-stress or 1CT-rest) for AC of gated rest-stress MP SPECT with Tc-99m sestamibi in quantification of myocardial perfusion and LV function values. This allowed us to evaluate the reliability of using just one CT for AC instead of two. Elimination of an extra CT for AC without affecting the myocardial perfusion and LV function values obtained from gated rest-stress MP SPECT could reduce patients' radiation exposure without having any impact on diagnostic results. Even though patients receive only a small amount of radiation exposure from CT for AC (0.4 mSv) [28], eliminating one CT for AC should be considered, in accordance with the principle of keeping radiation exposure as low as reasonably achievable (ALARA).

Several previous studies have examined the effectiveness of using one CT for AC of rest and stress MP SPECT in quantification of myocardial perfusion values such as SRS, SSS and SDS. Ahlman et al. [24] found that a single rest or stress CT was not sufficient for AC of both rest and stress MP SPECT; however, their study adopted a small number of patients (40) with abnormal perfusion only, and it included a mixture of patients who underwent thallium-201 (^{201}Tl)/ ^{99m}Tc (dual isotope) and ^{99m}Tc/^{99m}Tc (single isotope) one-day rest/stress protocols. The ^{99m}Tc emits gamma rays with single energy of 140 keV while ^{201}Tl emits smaller numbers of gamma rays at energies of 135 keV and 167 keV. The attenuation effects of ^{201}Tl and ^{99m}Tc may vary as a result of their different energies; therefore, it may be difficult to compare the use of one and two CTs for AC in a mixture of dual isotope and single isotope protocols.

Wells et al. [25] studied the use of a single CT, choosing stress CT for AC of both rest and stress MP SPECT. Their study included 154 patients who underwent one-day rest/stress MP SPECT with Tc-99m tetrofosmin, and they found that the use

THE ASEAN JOURNAL OF RADIOLOGY
ISSN 2672-9393

of stress CT for AC of both rest and stress SPECT images caused a significant increase in SRS and a rise in the variability of SDS compared with the use of two CTs. However, the variability in SDS between the use of one and two CTs was seen to be less than the inter-observer variability, suggesting that the differences resulting from one CT are unlikely to be clinically significant.

Fukami et al. [26] examined the effectiveness of the single CTAC method in gated stress-rest MP SPECT with ^{201}Tl-chloride (^{201}TlCl) in 106 patients. Like Wells et al., they chose stress CT (rather than rest CT) for AC comparison, with two CTs for AC. They concluded that there was no significant difference between SRS, SSS and SDS obtained by two CTs and a single CT.

Unlike Fukami et al., we studied gated stress-rest MP SPECT with Tc-99m sestamibi. The Tc-99m sestamibi MP SPECT provides significantly better image quality and higher specificity in detection of CAD than ^{201}TlCl MP SPECT [29]. In addition, we compared 3 different CTAC methods: 2CT, 1CT-rest and 1CT-stress. However, the results of Wells's study, Fukami's study and our study in comparing 2CT and 1CT-stress were similar. Our results showed that there was a strong correlation between SRS, SSS and SDS obtained by 2CT and 1CT with no significant differences. Therefore, 1CT and 2CT can be used interchangeably for the quantification of MP values. Because SDS can be clinically used to diagnose the degree of ischemia [8], we have conducted further studies regarding the diagnosis of myocardial ischemia using SDS values. In our study, the concordance of diagnostic results based on the SDS between 2CT and 1CT-stress was high: 91.7% for patients with no ischemia, 91.3% for patients with mild ischemia, 100% for patients with severe ischemia, and 88.8% for all patients except those with moderate ischemia, resulting in a diagnostic concordance of 58.3%. The concordance of diagnostic results based on the SDS from 2CT and 1CT-rest was quite high but lower than that achieved by 2CT and 1CT-stress: 75.0% for patients with no ischemia, 71.7% for patients with mild ischemia, 69.2% for patients with severe ischemia, and 68.2% for all patients except those with moderate ischemia, yielding a diagnostic concordance of 33.3%. These results suggest that using stress CT for AC is better than using rest CT for AC of both rest and stress SPECT.

Although the concordance of diagnostic results based on the SDS between 2CT and 1CT was relatively high, there are still some differences in diagnostic results among certain patients, especially those with moderate ischemia. The SDS was calculated from the SRS and SSS. Therefore, if the SRS and SSS obtained from 2CT and 1CT were different, it affected the SDS value and diagnostic results based on the SDS. When interpreting diagnostic results based on the SDS, if a patient falls into the category of moderate ischemia, which lies between mild ischemia and severe ischemia, even a slight difference in SDS values obtained from 2CT and 1CT can lead to divergent diagnostic results. However, the comparison of 1CT and 2CT for the diagnosis of myocardial ischemia from ^{99m}Tc-sestamibi rest-stress MP SPECT should be further investigated using visual inspection of SPECT images by nuclear medicine radiologists. Other myocardial perfusion values, such as rest TPD, stress TPD and TID, were included in our study, and no statistically significant difference was identified between myocardial perfusion values from 2CT and 1CT. These results suggest that 1CT can be used in place of 2CT in quantification of myocardial perfusion values from ^{99m}Tc-sestamibi rest-stress MP SPECT imaging. The use of stress CT for the 1CT approach revealed that the variability between SDS from 1CT and 2CT was less than that resulting from using rest CT.

In addition to the myocardial perfusion values, we also studied LV function values including rest EDV, rest ESV, stress EDV, stress ESV, rest EF and stress EF. Fukami et al. compared EF from 2CT and 1CT, and their results showed no significant differences. In contrast, our results revealed statistically significant differences in rest EF, stress EF and other LV function values obtained from 2CT and 1CT. However, the correlation between these LV function values obtained by 2CT and 1CT were very strong. The left ventricle EF was clinically used for assessment of the cardiac function [13]. In our study, the concordance of interpretation of LV function from rest EF between 2CT and 1CT was high: 87.5% for patients with reduced EF, 97.6% for patients with normal EF, and 93.5% for all patients except those with borderline EF, which yielded a concordance of interpretation of 50.0%. Regarding stress EF, the concordance of interpretation of the cardiac function between 2CT and 1CT was high: 100.0% for patients with reduced EF, 95.0% for

THE ASEAN JOURNAL OF RADIOLOGY
ISSN 2672-9393

patients with normal EF, and 92.5% for all patients except those with borderline EF, resulting in a concordance of interpretation of 66.7%. Even though interpreting the LV function from the EF values obtained from 1CT yielded similar results to those obtained from 2CT in more than 90% of patients, it can still lead to misinterpretations in patients with borderline EF values (41-49%).

Myocardial perfusion values were obtained from non-gated SPECT data while LV function values were derived from gated SPECT data. The LV function values from 2CT and 1CT were significantly different. The myocardial perfusion values from 2CT and 1CT were not significantly different, but these values obtained from 2CT and 1CT were not equal in all patients. This can be caused by a change in the distribution of attenuating tissues between SPECT and CT acquisitions in both rest and stress image sessions. Mis-registration of CT and SPECT images can cause an error in attenuation correction and influence regional tracer distribution on MP SPECT images [30]. This error may be due to changes in the patient position, the movement of arms, the movement of gas in the bowel, as well as the respiratory and cardiac motion during and between image acquisitions in rest-stress MP SPECT/CT imaging. Differences in the cardiac motion and the respiratory motion between patients who underwent exercise stress (resulting in an increased heart rate and contractility) and patients who underwent pharmacologic stress with adenosine (which causes vasodilation in coronary vessels) [31] may also result in a varying degree of mis-registration of SPECT and CT images. CT yields rapid acquisition while SPECT is slower, with free breathing. Stress and rest CT images may be acquired in different phases of the cardiac and respiratory cycles, and the aforementioned events may lead to a mismatch of attenuating tissues and errors in attenuation correction, which is applied at a single time point in the cardiac and respiratory cycles. It is, therefore, very important to set exactly the same patient positions and minimize the patient motion as much as possible during and between the image acquisitions, especially when using one CT for AC. In our study, automated fusion of SPECT and CT was used, and then alignment of the SPECT and CT images was visually confirmed. In case of misalignment between the images, the CT image was shifted to match the borders of the left ventricle in the SPECT image. Apart from attenuation, scatter is another factor affecting quantitative values obtained from MP SPECT images. The model-based

and energy-window-based methods are widely-used scatter correction techniques in MP SPECT imaging [32, 33]. The first method uses an attenuation map from CT to define the scattering medium. With this method, the mis-registration of SPECT and CT images and error in attenuation correction will also lead to inaccurate scatter correction [25]. Instead of using transmission (CT) data, the energy-window-based technique uses scatter data acquired simultaneously with that of photopeak emission. In our study, we used energy-window-based scatter correction, which is likely to be more suitable for the use of one CT for AC in rest-stress MP SPECT imaging.

The main limitations of this study were that we processed gated rest-stress MP SPECT data retrospectively, and that the proportion of normal and abnormal patients were not equal. This study used image data from patients who underwent rest-stress MP SPECT/CT without separating patient data between those who underwent exercise stress and those who underwent pharmacological stress. We used automated quantitative values (rather than qualitative or visual interpretation) for the statistical analysis to eliminate inter-individual variability of MP SPECT interpretation; thus, visual interpretation, which is used in many institutions, was not included in this study.

Conclusion

The myocardial perfusion values from 2CT and 1CT were not significantly different and exhibited a strong correlation. When using stress CT for the 1CT approach, the variability in SDS from 1CT and 2CT was observed to be less than that resulting from using rest CT. However, the comparison of 1CT and 2CT for the diagnosis of myocardial ischemia from ^{99m}Tc-sestamibi rest-stress MP SPECT should be further investigated using visual inspection of SPECT images by nuclear medicine radiologists. The LV function values from 2CT and 1CT exhibited a very strong correlation but were significantly different. In conclusion, the use of one and two CTs for AC in rest-stress MP SPECT with Tc-99m sestamibi can be interchanged for the quantification of myocardial perfusion, but not for the quantification of LV function.

References

1. Bateman TM, Cullom SJ. Attenuation correction single-photon emission computed tomography myocardial perfusion imaging. Semin Nucl Med 2005;35:37-51. doi: 10.1053/j.semnuclmed.2004.09.003.

2. Jaarsma C, Leiner T, Bekkers SC, Crijns HJ, Wildberger JE, Nagel E, et al. Diagnostic performance of noninvasive myocardial perfusion imaging using single-photon emission computed tomography, cardiac magnetic resonance, and positron emission tomography imaging for the detection of obstructive coronary artery disease: a meta-analysis. J Am Coll Cardiol 2012;59:1719-28. doi: 10.1016/j.jacc.2011.12.040.

3. Rischpler C, Nekolla S, Schwaiger M. PET and SPECT in heart failure. Curr Cardiol Rep 2013;15:337. doi: 10.1007/s11886-012-0337-z.

4. Cremer P, Hachamovitch R, Tamarappoo B. Clinical decision making with myocardial perfusion imaging in patients with known or suspected coronary artery disease. Semin Nucl Med 2014;44:320-9. doi: 10.1053/j.semnuclmed.2014.04.006.

5. Kostkiewicz M. Myocardial perfusion imaging in coronary artery disease. Cor et Vasa 2015;57:e446-52.

6. Lehner S, Nowak I, Zacherl M, Brosch-Lenz J, Fischer M, Ilhan H, et al. Quantitative myocardial perfusion SPECT/CT for the assessment of myocardial tracer uptake in patients with three-vessel coronary artery disease: initial experiences and results. J Nucl Cardiol 2022;29:2511-20. doi: 10.1007/s12350-021-02735-2.

7. Strauss HW, Miller DD, Wittry MD, Cerqueira MD, Garcia EV, Iskandrian AS, et al. Procedure guideline for myocardial perfusion imaging 3.3. J Nucl Med Tech 2008;36:155-61. doi: 10.2967/jnmt.108.056465.

8. Czaja M, Wygoda Z, Duszańska A, Szczerba D, Głowacki J, Gąsior M, et al. Interpreting myocardial perfusion scintigraphy using single-photon emission computed tomography. Part 1. Kardiochir Torakochirurgia Pol 2017;14:192-9. doi: 10.5114/kitp.2017.70534.

9. Abidov A, Germano G, Hachamovitch R, Slomka P, Berman DS. Gated SPECT in assessment of regional and global left ventricular function: an update. J Nucl Cardiol 2013;20:1118-43. doi: 10.1007/s12350-013-9792-1.

10. Go V, Bhatt MR, Hendel RC. The diagnostic and prognostic value of ECG-gated SPECT myocardial perfusion imaging. J Nucl Med 2004;45:912-21.

11. Slart RH, Tio RA, Zeebregts CJ, Willemsen A, Dierckx RA, De Sutter J. Attenuation corrected gated SPECT for the assessment of left ventricular ejection fraction and volumes. Ann Nucl Med 2008;22:171-6. doi: 10.1007/s12149-007-0100-5.

12. Bavelaar-Croon CD, Kayser HW, van der Wall EE, de Roos A, Dibbets-Schneider P, Pauwels EK, et al. Left ventricular function: correlation of quantitative gated SPECT and MR imaging over a wide range of values. Radiology 2000; 217:572-5. doi: 10.1148/radiology.217.2.r00nv15572.

13. Czaja MZ, Wygoda Z, Duszańska A, Szczerba D, Głowacki J, Gąsior M, et al. Myocardial perfusion scintigraphy-interpretation of gated imaging. Part 2. Kardiochir Torakochirurgia Pol 2018;15:49-56. doi: 10.5114/kitp.2018.74676.

14. Hendel RC, Corbett JR, Cullom SJ, DePuey EG, Garcia EV, Bateman TM. The value and practice of attenuation correction for myocardial perfusion SPECT imaging: a joint position statement from the American Society of Nuclear Cardiology and the Society of Nuclear Medicine. J Nucl Cardiol 2002;9:135-43. doi: 10.1067/mnc.2002.

15. Burrell S, MacDonald A. Artifacts and pitfalls in myocardial perfusion imaging. J Nucl Med Technol 2006;34:193-211 ; quiz 212-4.

THE ASEAN JOURNAL OF RADIOLOGY
ISSN 2672-9393

16. Singh B, Bateman TM, Case JA, Heller G. Attenuation artifact, attenuation correction, and the future of myocardial perfusion SPECT. J Nucl Cardiol 2007; 14:153-64. doi: 10.1016/j.nuclcard.2007.01.037.

17. Slart RH, Que TH, van Veldhuisen DJ, Poot L, Blanksma PK, Piers DA, et al. Effect of attenuation correction on the interpretation of 99mTc-sestamibi myocardial perfusion scintigraphy: the impact of 1 year's experience. Eur J Nucl Med Mol Imaging 2003;30:1505-9. doi: 10.1007/s00259-003-1265-3.

18. Masood Y, Liu YH, Depuey G, Taillefer R, Araujo LI, Allen S, et al. Clinical validation of SPECT attenuation correction using x-ray computed tomography-derived attenuation maps: multicenter clinical trial with angiographic correlation. J Nucl Cardiol 2005;12:676-86. doi: 10.1016/j.nuclcard.2005.08.006.

19. Garcia EV. SPECT attenuation correction: an essential tool to realize nuclear cardiology's manifest destiny. J Nucl Cardiol 2007;14:16-24. doi: 10.1016/j.nuclcard.2006.12.144.

20. Huang JY, Huang CK, Yen RF, Wu HY, Tu YK, Cheng MF, et al. Diagnostic performance of attenuation-corrected myocardial perfusion imaging for coronary artery disease: a systematic review and meta-analysis. J Nucl Med 2016;57:1893-8. doi: 10.2967/jnumed.115.171462.

21. Cerqueira MD, Allman KC, Ficaro EP, Hansen CL, Nichols KJ, Thompson RC, et al. Recommendations for reducing radiation exposure in myocardial perfusion imaging. J Nucl Cardiol 2010;17:709-18. doi: 10.1007/s12350-010-9244-0.

22. Einstein AJ. Multiple opportunities to reduce radiation dose from myocardial perfusion imaging. Eur J Nucl Med Mol Imaging 2013;40:649-51. doi: 10.1007/s00259-013-2355-5.

23. Ahlman MA, Suranyi P, Spicer KM, Gordon L. Comparison of one vs two CTs for attenuation correction of both rest and stress SPECT data for myocardial perfusion imaging with Tc-99m Tetrofosmin. J Nucl Med 2011;52:1129.

24. Ahlman MA, Nietert PJ, Wahlquist AE, Serguson JM, Berry MW, Suranyi P, et al. A single CT for attenuation correction of both rest and stress SPECT myocardial perfusion imaging: a retrospective feasibility study. Int J Clin Exp Med 2014;7:148-55.

25. Wells RG, Trottier M, Premaratne M, Vanderwerf K, Ruddy TD. Single CT for attenuation correction of rest/stress cardiac SPECT perfusion imaging. J Nuclear Cardiol 2018;25:616-24. doi: 10.1007/s12350-016-0720-z.

26. Fukami M, Tamura K, Nakamura Y, Nakatsukasa S, Sasaki M. Evaluating the effectiveness of a single CT method for attenuation correction in stress-rest myocardial perfusion imaging with thallium-201 chloride SPECT. Radiol Phys Technol 2020;13:20-6. doi: 10.1007/s12194-019-00540-8.

27. Slomka PJ, Berman DS, Germano G. Normal limits for transient ischemic dilation with 99mTc myocardial perfusion SPECT protocols. J Nucl Cardiol 2017;24:1709-11. doi: 10.1007/s12350-016-0582-4.

28. Preuss R, Weise R, Lindner P, Fricke E, Fricke H, Burchert W. Optimisation of protocol for low dose CT-derived attenuation correction in myocardial perfusion SPECT imaging. Eur J Nucl Med Mol Imaging 2008;35:1133-41. doi: 10.1007/s00259-007-0680-2.

29. Taillefer R, DePuey EG, Udelson JE, Beller GA, Latour Y, Reeves F. Comparative diagnostic accuracy of Tl-201 and Tc-99m sestamibi SPECT imaging (perfusion and ECG-gated SPECT) in detecting coronary artery disease in women. J Am Coll Cardiol 1997;29:69-77. doi: 10.1016/s0735-1097(96)00435-4.

30. Goetze S, Brown TL, Lavely WC, Zhang Z, Bengel FM. Attenuation correction in myocardial perfusion SPECT/CT: effects of misregistration and value of reregistration. J Nucl Med 2007;48:1090-5. doi: 10.2967/jnumed.107.040535.

THE ASEAN JOURNAL OF RADIOLOGY
ISSN 2672-9393

31. Henzlova MJ, Duvall WL, Einstein AJ, Travin MI, Verberne HJ. ASNC imaging guidelines for SPECT nuclear cardiology procedures: stress, protocols, and tracers. J Nucl Cardiol 2016;23:606-39. doi: 10.1007/s12350-015-0387-x.

32. Hutton BF, Buvat I, Beekman FJ. Review and current status of SPECT scatter correction. Phys Med Biol 2011;56:R85-112. doi: 10.1088/0031-9155/56/14/R01.

33. Wells RG, Soueidan K, Timmins R, Ruddy TD. Comparison of attenuation, dual-energy-window, and model-based scatter correction of low-count SPECT to 82Rb PET/CT quantified myocardial perfusion scores. J Nucl Cardiol 2013;20:785-96. doi: 10.1007/s12350-013-9738-7.

Original Article

Body composition between obstructive and non-obstructive bladder cancer: A retrospective study

Apiwit Aphinives, M.D.
Supajit Nawapun, M.D.
Chalida Aphinives, M.D.
From Department of Radiology, Faculty of Medicine, Khon Kaen University, Thailand.
Address correspondence to A.A. (email: apiwap@kku.ac.th)

Received 23 January 2024; revised 22 June 2024; accepted 1 July 2024
doi:10.46475/asean-jr.v25i2.896

Abstract

Background: Body composition measurement during cancer follow-up would increase its role in improving the nutritional status. Using a CT scan for nutritional evaluation with scheduled cancer screening or follow-up would add other useful information to help the physician gain a better understanding of the patient's nutritional status, especially in adipose tissue.

Objective: To compare the measured adipose tissue and the skeletal muscle between obstructive and non-obstructive uropathy in bladder cancer on a CT scan.

Materials and methods: A total of 69 patients, who underwent a CT scan of the abdomen including the pelvis before surgery and/or chemotherapy between January 2013 and December 2022, were enrolled. Analyses of the volume of visceral adipose tissue (VAT), subcutaneous adipose tissue (SAT), and skeletal muscle tissue (SMT) calculated based on CT images were performed.

THE ASEAN JOURNAL OF RADIOLOGY
ISSN 2672-9393

Results: There was significantly lower VAT (p = 0.012) in the obstructive group than in the non-obstructive group. SAT, SMT, age, weight, height, BMI, and tumor size were not significantly different between both groups.

Conclusion: In patients with bladder cancer, those with obstructive uropathy showed lower VAT than non-obstructive uropathy.

Keywords: Bladder cancer, Body composition, Computed tomography, Skeletal muscle, Subcutaneous fat, Visceral fat.

Introduction

Urinary bladder cancer was the 10th most commonly diagnosed worldwide in 2020 and the 9th most common cancer in the Thai population (2.6%) [1]. The most common histology is urothelial carcinoma of the bladder, accounting for 90% of all urinary bladder cancers [2]. Cancer growth consumes massive energy. During progression, the patient usually loses appetite leading to anemia, poor immunity, weight loss, and cachexia. In a cachexic state, the patient would lose the body weight, the skeletal muscle, and the adipose tissue [3-4]. Cancer cachexia may half the quality of life, the mental health, the treatment response, and the survival [5].

Body mass index (BMI) is one of the fundamental indicators used to evaluate the nutritional status and cachexia, but only represents the total body composition and does not differentiate the ratio and alteration of fat and muscle mass. The muscle mass is significantly associated with the overall body condition and the nutritional status of cancer patients [6].

Body composition measurement during cancer follow-up would increase its role in improving the nutritional status. Because of the high price and the fact that it is rather time-consuming, some devices, such as Densitometry, MRI, TOBEC (total body electrical conductivity), and TBK (whole body potassium scanning), are hard to make a practical workflow in the situation of abundant patients on the same day [7].

Computed tomography (CT) is used for high-risk cancer patients or even an ongoing treatment to prove clinical suspicion and follow-up cancer progression or treatment response. It could show the whole body in the same period, vividly faster than the body composition measurement device. Using a CT scan for nutritional evaluation with scheduled cancer screening or follow-up would add other useful information to help the physician gain a better understanding of the patient's nutritional status, especially in adipose tissue [8-10].

The objective of this study was to compare the measured adipose tissue and skeletal muscle between obstructive and non-obstructive uropathy in bladder cancer on a CT scan.

Materials and methods

Ethical consideration

A retrospective descriptive diagnostic study was conducted at a university-based tertiary referral center in Thailand. The study was conducted following the Declaration of Helsinki, and the protocol was approved by the Ethics Committee for Human Research.

Study population

The medical records and CT scans of the abdomen including the pelvis of urinary bladder cancer patients from January 2013 to December 2022 were retrospectively reviewed. If patients underwent multiple studies of CT scan, the latest study prior to treatment was selected.

Inclusion criteria

1. Patients who were diagnosed with pathology-confirmed urinary bladder cancer
2. Patients who underwent CT scans of the abdomen including the pelvis

THE ASEAN JOURNAL OF RADIOLOGY
ISSN 2672-9393

Exclusion criteria

1. Patients who underwent a surgery and/or a chemotherapy before undergoing the CT scan
2. Patients who had a previous history of some other type of cancer or concomitant diagnosed cancer at the examined date

Hardware and data acquisition

All images were performed by SOMATOM Definition Flash (SIEMEN®) with and/or without intravenous contrast before the surgery. The protocol of CT whole abdomen (pre-contrast phase, arterial phase, and portovenous phase) or CT urography (pre-contrast phase, nephrographic phase, and excretory phase) were used. The slice thickness and interval ranged from 3 to 10 mm with a median of 5 mm.

3D Slicer 5.2.2 (www.slicer.org, The Slicer Community) was used to measure using a semiautomatic segmentation method. The images were separated into three main components: visceral adipose tissue (VAT), subcutaneous adipose tissue (SAT), and skeletal muscle tissue (SMT) [8].

Image interpretation

The definition of obstructive uropathy was defined as at least 3 mm of ureter diameter or unilateral or bilateral dilated ureter [11].

The CT attenuation value of adipose tissue was defined as -100 to -50 Hounsfield units (HUs). Three-dimensional (3D) volumes at the level of the costophrenic angle to the iliac crest and two-dimensional (2D) cross-section areas at the level of the third lumbar spine (L3) mid-vertebra were measured for VAT, SAT, and SMT [12-15].

Statistical analysis

Statistical analyses were performed using IBM SPSS v28.0.0.0 (IBM Corp., Armonk, NY, USA). The descriptive analysis was used for demographic data (such as gender, age, weight, height, etc.). Differences between obstructive and non-obstructive uropathy were performed using independent T-test or chi-square test (or Fisher's exact test as appropriate). A p-value < 0.05 was considered statistically significant.

Results

Out of 136 patients, 67 were excluded (27 for non-bladder cancers, 16 with concomitant cancers, and 24 without a pre-treatment study). Only 69 patients were eligible for enrollment. There were 57 patients with obstructive uropathy and 12 patients with non-obstructive uropathy.

Most patients were male with 48 (84%) in the obstructive group and 11 (92%) in the non-obstructive group. The mean age, height, BMI, and tumor size were not different between groups. More than half of the patients in both groups were in clinical stage III (Table 1).

Table 1. *Patients' demographic data.*

Parameters	Obstructive	Non-obstructive	p-value
Patients (Male : Female)	57 (48: 9)	12 (11: 1)	-
Age (Years)	65.4 + 9.9	70.5 + 9.0	0.590
Weight (kg)	60.5 + 10.6	60.8 + 10.7	0.737
Height (cm)	163.3 + 7.6	164.3 + 7.8	0.798
BMI (kg/m^2)	22.7 + 3.9	22.4 + 3.1	0.522
Tumor size (cm^3)	34.4 + 84.0	38.5 + 87.6	0.770
Clinical stage I	0 (0%)	0 (0%)	N/A
Clinical stage II	1 (1.7%)	3 (25%)	0.015
Clinical stage III	37 (64.9%)	7 (58.3%)	0.746
Clinical stage IV	19 (33.3%)	2 (16.7%)	0.321

A body composition analysis was performed using a semiautomatic segmentation, 3-dimensional (3D) volume at the level of the costophrenic angle to the iliac crest, and 2-dimensional (2D) cross-section areas at the level of 3rd lumbar spine (L3) (Figure 1).

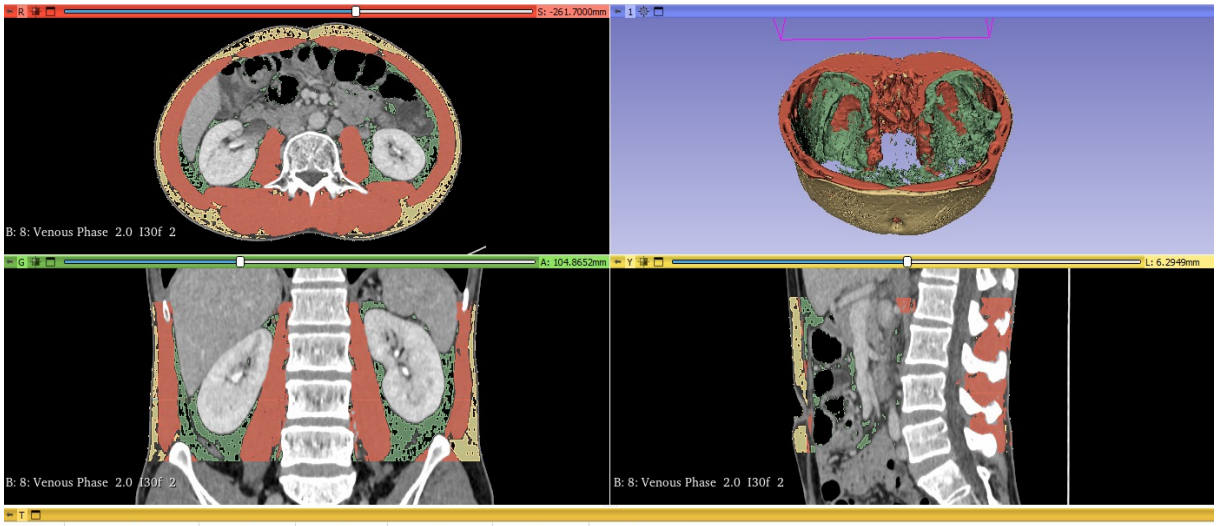

	A	B	C	D	E	F	G
1	**Segment**	**Number of voxels [voxels]**	**Volume [mm3] (1)**	**Volume [cm3] (1)**	**Surface area [mm2]**	**Volume [mm3] (2)**	**Volume [cm3] (2)**
2	VAT	1696603	590275	590.275	440272	570077	570.077
3	SAT	991712	345032	345.032	238693	345026	345.026
4	VAT (L3)	4753	1653.64	1.65364	1962.52	461.614	0.461614
5	SAT (L)	8739	3040.43	3.04043	4442.85	1220.97	1.22097
6	SMT	3901949	1.35755e+06	1357.55	278507	1.36342e+06	1363.42
7	SMT (L3)	34075	11855.2	11.8552	23016.7	10805.1	10.8051

Figure 1. *Example of abdominal computed tomography for body composition analysis (upper left: axial plane, lower left: coronal plane, lower right: sagittal plane, upper right: 3D model, bottom: measured variables in 3D and 2D at the level of L3). Visceral adipose tissue (green), subcutaneous adipose tissue (yellow), and skeletal muscle tissue (red) were segmented.*

The mean VAT volume in the obstructive group was 851.9 cm^3, which is significantly lower than the non-obstructive group (mean = 1137.9 cm^3, p = 0.012). Other variables showed no statistically significant difference between groups (Table 2).

Table 2. *Significant difference analysis between obstructive and non-obstructive uropathy.*

Parameters	Obstructive (Mean + SD)	Non-obstructive (Mean + SD)	p-value
BMI (kg/m^2)	22.7 + 3.9	22.4 + 3.1	0.522
VAT (cm^3)	851.9 + 579.8	1137.9 + 579.8	0.012*
SAT (cm^3)	758.9 + 459.7	756.3 + 395.5	0.884
VAT-L3 (cm^2)	76.7 + 67.4	86.3 + 99.9	0.266
SAT-L3 (cm^2)	66.2 + 122.5	59.8 + 67.0	0.811
SMT (cm^3)	1493.2 + 419.2	1542.4 + 419.2	0.461
SMT-L3 (cm^2)	213.2 + 59.2	215.7 + 65.9	0.454
Tumor volume (cm^3)	34.4 + 84.0	38.5 + 87.6	0.770

**Statistical significance*

Discussion

There was no report of a correlation between obstructive and non-obstructive uropathy in bladder cancer that was measured by computed tomography [12-15]. There was one systematic review that collected related bladder cancer [9]. Previous studies were focused on a prognosis and the clinical outcome between pre-treatment and post-treatment with a multi-treatment plan by skeletal muscle index [16-19]. There was no study focusing on the correlation between variables in pre-treatment patients.

From the result, the VAT showed a statistic significance between obstructive and non-obstructive uropathy but not in the SAT which showed a similar result to previous studies [8]. Also, it was compatible with the previous meta-analysis studies or hypothesis that VAT was more vulnerable to prognosis than SAT or even BMI [9]. The obstructive group presented with lower VAT which was compatible with clinical prognosis revealing that obstructive uropathy tended to have a worse clinical outcome compared to the non-obstructive group. Lastly, the VAT showed more sensitive differences in patients' nutritional status than BMI [8, 12-15].

THE ASEAN JOURNAL OF RADIOLOGY
ISSN 2672-9393

Obstructive uropathy was an obstruction of the urinary tract that could be caused by either structural or functional problem. The obstruction could present with typical combination of micturition, acute urinary retention, or lower abdominal discomfort and distension [20]. Untreated obstructive uropathy would eventually lead to chronic kidney damage or a disease that could reduce muscle mass via spontaneous reduction of albumin absorption [21].

The living quality of the patients with obstructive uropathy would be a vicious cycle as dysuria leads to nocturia, causes inadequate sleep, deterioration, and fatigue that causes dysuria again which is a cause of an excessive power expenditure over nights [22]. Combined with malnutrition, the insufficient energy to maintain daily activity forces the body to use the reserved tissue to survive [23].

Adipose tissue is a primary source of nutrition with a rapid process of lipolysis for turning the fat into glycerol for gluconeogenesis and ketone bodies as a direct fuel source for many tissues, including the brain. Also, it is the first in the three phases of response to the deprivation of nutrition. When fat depots are depleted, the skeletal muscle will be degraded by proteolysis to support the gluconeogenesis in the liver. In this situation, the body mass will rapidly decrease that can be shown in the reduction of BMI [24-25].

Further studies should be conducted with multiple hospitals to enroll sufficient patients to make the data solid. A comparison between groups of obstructive and non-obstructive uropathy with localized and metastatic cancers could potentially specify the prognosis that could create adequate data for clinicians to better understand patients' status and treatment planning, not only in the disease control but also in the overall quality of life.

Several limitations need to be considered when interpreting the results. The retrospective nature of the small sample size in the single-center study might lead to a selection bias and lower the confidence of the result. Non-structural records in the hospital digital clinical data and partially paper-based clinicians might contribute lower than the actual number of patients.

Conclusion

To our knowledge, this is the first study to have evaluated the difference in body composition of patients with urinary bladder cancer affected by obstructive uropathy. Obstructive uropathy showed lower VAT than non-obstructive uropathy.

References

1. Sung H, Ferlay J, Siegel RL, Laversanne M, Soerjomataram I, Jemal A, et al. Global cancer statistics 2020: GLOBOCAN estimates of incidence and mortality worldwide for 36 cancers in 185 countries. CA Cancer J Clin 2021;71:209–49. doi: 10.3322/caac.21660.

2. Antoni S, Ferlay J, Soerjomataram I, Znaor A, Jemal A, Bray F. Bladder cancer incidence and mortality: A global overview and recent trends. Eur Urol 2017;71:96–108. doi: 10.1016/j.eururo.2016.06.010.

3. Baracos VE, Martin L, Korc M, Guttridge DC, Fearon KCH. Cancer-associated cachexia. Nat Rev Dis Primers 2018;4:17105. doi: 10.1038/nrdp.2017.105.

4. Grimberg DC, Shah A, Molinger J, Whittle J, Gupta RT, Wischmeyer PE, et al. Assessments of frailty in bladder cancer. Urol Oncol 2020;38:698–705. doi: 10.1016/j.urolonc.2020.04.036.

5. Fukushima H, Takemura K, Suzuki H, Koga F. Impact of sarcopenia as a prognostic biomarker of bladder cancer. Int J Mol Sci 2018;19:2999. doi: 10.3390/ijms19102999.

6. Tanaka K, Taoda A, Kashiwagi H. The associations between nutritional status, physical function and skeletal muscle mass of geriatric patients with colorectal cancer. Clin Nutr ESPEN 2021;41:318–24. doi: 10.1016/j.clnesp.2020.11.009.

THE ASEAN JOURNAL OF RADIOLOGY
ISSN 2672-9393

7. Wells JC, Fewtrell MS. Measuring body composition. Arch Dis Child 2005;91: 612–7. doi: 10.1136/adc.2005.085522.

8. Tan CC, Sheng TW, Chang YH, Wang LJ, Chuang CK, Wu CT, et al. Utilizing computed tomography to analyze the morphomic change between patients with localized and metastatic renal cell carcinoma: body composition varies according to cancerstage. J Clin Med 2022;11:4444. doi: 10.3390/jcm11154444.

9. Sanchez A, Kissel S, Coletta A, Scott J, Furberg H. Impact of body size and body composition on bladder cancer outcomes: Risk stratification and opportunity for novel interventions. Urol Oncol 2020 ;38:713–8. doi: 10.1016/j.urolonc.2020.03.017.

10. Borga M, West J, Bell JD, Harvey NC, Romu T, Heymsfield SB, et al. Advanced body composition assessment: from body mass index to body composition profiling. J Invest Med 2018;66:1–9. doi: 10.1136/jim-2018-000722.

11. Potenta SE, D'Agostino R, Sternberg KM, Tatsumi K, Perusse K. CT urography for evaluation of the ureter. Radiographics 2015;35:709–26. doi: 10.1148/rg.2015140209.

12. Zhao L, Tian X, Duan X, Ye Y, Sun M, Huang J. Association of body mass index with bladder cancer risk: a dose-response meta-analysis of prospective cohort studies. Oncotarget 2017;8:33990–4000. doi: 10.18632/oncotarget.16722.

13. Rigiroli F, Zhang D, Molinger J, Wang Y, Chang A, Wischmeyer PE, et al. Automated versus manual analysis of body composition measures on computed tomography in patients with bladder cancer. Eur J Radiol 2022; 154:110413. doi: 10.1016/j.ejrad.2022.110413.

14. Franco-Villoria M, Wright CM, McColl JH, Sherriff A, Pearce MS; Gateshead Millennium Study core team. Assessment of adult body composition using bioelectrical impedance: comparison of researcher calculated to machine outputted values. BMJ Open 2016;6:e008922. doi: 10.1136/bmjopen-2015-008922.

15. Ying T, Borrelli P, Edenbrandt L, Enqvist O, Kaboteh R, Trägårdh E, et al. Automated artificial intelligence-based analysis of skeletal muscle volume predicts overall survival after cystectomy for urinary bladder cancer. Eur Radiol Exp 2021;5:50. doi: 10.1186/s41747-021-00248-8.

16. Miyake M, Morizawa Y, Hori S, Marugami N, Shimada K, Gotoh D, et al. Clinical impact of postoperative loss in psoas major muscle and nutrition index after radical cystectomy for patients with urothelial carcinoma of the bladder. BMC Cancer 2017;17237. doi: 10.1186/s12885-017-3231-7

17. Miyake M, Owari T, Iwamoto T, Morizawa Y, Hori S, Marugami N, et al. Clinical utility of bioelectrical impedance analysis in patients with locoregional muscle invasive or metastatic urothelial carcinoma: a subanalysis of changes in body composition during neoadjuvant systemic chemotherapy. Support Care Cancer 2018;26:1077–86. doi: 10.1007/s00520-017-3924-0.

18. Phuong A, Marquardt JP, O'Malley R, Holt SK, Laidlaw G, Eagle Z, et al. Changes in skeletal muscle and adipose tissue during cytotoxic chemotherapy for testicular germ cell carcinoma and associations with adverse events. Urol Oncol 2022;40:456.e19-456.e30. doi: 10.1016/j.urolonc.2022.07.013.

19. Stangl-Kremser J, D'Andrea D, Vartolomei M, Abufaraj M, Goldner G, Baltzer P, et al. Prognostic value of nutritional indices and body composition parameters including sarcopenia in patients treated with radiotherapy for urothelial carcinoma of the bladder. Urol Oncol 2019;37:372–9. doi: 10.1016/j.urolonc.2018.11.001.

20. Rishor-Olney CR, Hinson MR. Obstructive uropathy. [Updated 2023 Jul 22]. In: StatPearls [Internet]. Treasure Island (FL): StatPearls Publishing; 2024 Jan- [cited 2024 Jul 4]. Available from: http://www.ncbi.nlm.nih.gov/books/NBK558921/

THE ASEAN JOURNAL OF RADIOLOGY
ISSN 2672-9393

21. Jensen GL. Malnutrition and nutritional assessment. In: Loscalzo J, Fauci A, Kasper D, Hauser S, Longo D, Jameson J, editors. Harrison's principles of internal medicine [Internet]. 21th ed. McGraw Hill; 2022 [cited 2024 Jul 4]. Available from: https://accessmedicine.mhmedical.com/content.aspx?bookid=3095&sectionid=264532265

22. Ancoli-Israel S, Bliwise DL, Nørgaard JP. The effect of nocturia on sleep. Sleep Med Rev 2011;15:91–7. doi: 10.1016/j.smrv.2010.03.002.

23. Wensveen FM, Valentić S, Šestan M, Turk Wensveen TT, Polić B. Interactions between adipose tissue and the immune system in health and malnutrition. Semin Immunol2015;27:322–33. doi: 10.1016/j.smim.2015.10.006.

24. Lyon TD, Frank I, Takahashi N, Boorjian SA, Moynagh MR, Shah PH, et al. Sarcopenia and response to neoadjuvant chemotherapy for muscle-invasive bladder cancer. Clin Genitourin Cancer 2019;17:216-22.e5. doi: 10.1016/j.clgc.2019.03.007.

25. Wang Y, Chang A, Tan WP, Fantony JJ, Gopalakrishna A, Barton GJ, et al. Diet and exercise are not associated with skeletal muscle mass and sarcopenia in patients with bladder cancer. Eur Urol Oncol 2021;4:237–45. doi: 10.1016/j.euo.2019.04.012.

Case Report

Fatty menace: A case report of superior ophthalmic vein fat embolism due to autologous fat grafting

Sirote Wongwaisayawan, M.D.
Pinporn Jenjitranant, M.D.
From Department of Diagnostic and Therapeutic Radiology, Faculty of Medicine Ramathibodi Hospital Mahidol University, Bangkok, Thailand.
Address correspondence to S.W. (e-mail: sirote.won@mahidol.edu)

Received 16 April 2024; revised 25 July 2024; accepted 30 July 2024
doi:10.46475/asean-jr.v25i2.904

Abstract

Autologous fat grafting is among the many procedures used for facial rejuvenation and reconstruction, and its popularity has been increasing in Asia and worldwide. This procedure carries a risk of arterial or venous occlusion, which can lead to serious consequences. Venous embolism following autologous fat grafting is rarely reported. Here, we present a case of superior ophthalmic vein fat embolism and orbital compartment syndrome in a patient who underwent autologous fat grafting. Timely diagnosis, appropriate referral, and comprehensive multidisciplinary assessment are crucial for achieving favorable clinical outcomes.

Keywords: Autologous fat grafting, Fat embolism, Orbital compartment syndrome, Superior ophthalmic vein.

THE ASEAN JOURNAL OF RADIOLOGY
ISSN 2672-9393

Introduction

Autologous fat grafting has been increasingly used in Asia and worldwide for facial rejuvenation and reconstruction. Despite the familiarity with this technique, many complications have been reported, including facial edema and ecchymosis, cellulitis and granuloma, skin irregularities, skin blistering, scarring, and vascular complications [1-4]. Isolated venous fat embolism following autologous fat grafting is rarely mentioned. This case report presents a rare case of superior ophthalmic vein fat embolism and orbital compartment syndrome due to autologous fat grafting.

Case summary

A healthy 38-year-old female presented to our emergency department (ED) with a sudden onset of pain, swelling, and a blurred vision in her right eye for the past 3 hours. Upon taking her medical history, it was revealed that she had undergone autologous fat grafting at a clinic. Approximately 45 ml of fat graft were harvested and injected into bilateral temporal and right periorbital areas. The symptoms began to manifest about 2 hours after the procedure. She denied a history of previous surgery or trauma.

Upon arrival, she was fully conscious, and her vital signs were within normal limits. A physical examination of her right eye revealed a visual acuity (VA) of 20/70, an intraocular pressure (IOP) of 53 mmHg, and a negative relative afferent pupillary defect (RAPD). Additionally, she had chemosis, injected conjunctiva, and limited upward and downward gaze. The physical examination of her left eye yielded normal results, and her neurologic examination was also normal.

Emergency CT venography of the orbit was performed. The CTV revealed a tubular-shaped fat-attenuation (-60 Hounsfield unit; HU) filling defect in the dilated right superior ophthalmic vein, along with right intraconal fat stranding, right proptosis, stretching of the right optic nerve, and engorgement of the right extraocular muscles (Figure 1). Based on her clinical presentation and CT findings, a diagnosis

of superior ophthalmic vein fat embolism and orbital compartment syndrome was established. Ophthalmologists and interventional neuroradiologists were consulted to participate in the patient's care.

Figure 1. *Axial (A and B) and coronal-reformatted (C) CTV images show a dilated right superior ophthalmic vein with intraluminal fat-attenuation (-60 HU) filling defect (red arrows in A and C). Additionally, right eye proptosis, right retrobulbar fat stranding, stretching of the right optic nerve, and engorgement of the right extraocular muscles are noted, suggesting orbital congestion.*

The initial treatment consisted of 250 mg of oral acetazolamide followed by 250 mg every 6 hours, 50 ml of 50% oral glycerol followed by 80 ml every 8 hours, brimonidine 0.2% ophthalmic solution every 12 hours, and timolol 0.5% ophthalmic solution every 12 hours. Unfortunately, there was no improvement in her VA and IOP after the medical treatment. Consequently, lateral canthotomy and inferior cantholysis were performed. Shortly after the surgery, her right eye VA improved to 20/20, and the IOP of the right eye was 16 mmHg. She also reported an improvement in right eye pain. As a result, the planned endovascular treatment with transvenous embolectomy was postponed. Additionally, 1000 mg of intravenous methylprednisolone was administered, followed by oral prednisolone at 50 mg per day for two weeks. She was discharged without any complications after 5 days of hospitalization. At the three-month follow-up, she had achieved complete clinical recovery, denying any blurred vision or eye pain. Her right eye VA remained at 20/20, and the right eye IOP was 15 mmHg. Follow-up CTV at 3 months (Figure 2) revealed decreased filling defects in the right superior ophthalmic vein and resolution of right orbital congestion.

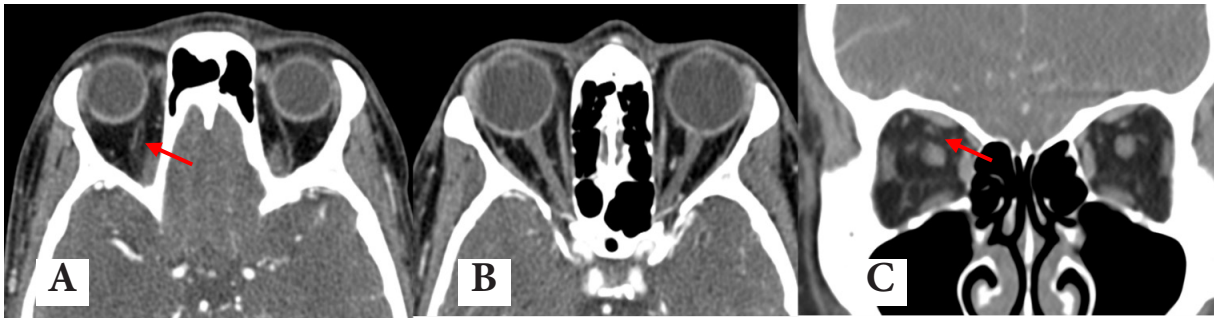

Figure 2. *Axial (A and B) and coronal-reformatted (C) CTV images at 3-month follow-up show decreased filling defect in the right superior ophthalmic vein (red arrows in A and C). Also note resolution of right orbital congestion.*

Discussion

Autologous fat grafting, also referred to as autologous fat injection or transfer, is a procedure that involves harvesting adipose tissue from areas like the flank, inner thigh, or abdomen, and then injecting it into recipient sites at desirable locations. This technique is one of many procedures used for facial rejuvenation and reconstruction, and its popularity has been increasing in Asia and globally [5].

Despite the favorable outcomes of this technique, many complications of autologous fat grafting have been reported. These complications include facial edema and ecchymosis, cellulitis, granuloma, skin irregularities, skin blistering, and scarring. In some cases, the patient may suffer blindness or stroke due to the retrograde movement of fat particles into the ophthalmic artery, central retinal artery, and internal carotid artery [1-4]. Isolated venous fat embolism following autologous fat grafting is rarely reported [6]. The embolized fat particle may cause mechanical obstruction of the vessel (macroscopic fat embolism) or trigger an inflammatory cascade, resulting in local blood vessel damage and endothelial injury (microscopic fat embolism) [7].

To the best of our knowledge, there is no published literature regarding orbital compartment syndrome as a complication of autologous facial fat grafting. We

propose that a macroscopic fat particle caused a blockage in the superior ophthalmic vein, which serves as an outflow venous drainage of the orbit. This blockage resulted in orbital congestion and a subsequent rise in intraorbital pressure. Given that the orbit is a closed conical space surrounded by bony walls, it is highly susceptible to any sudden increase in pressure, which can lead to impaired perfusion and ischemia of the optic nerve and retina.

Symptoms of orbital compartment syndrome include impaired VA, marked proptosis, and evidence of increased intraorbital pressure. Diagnosis of orbital compartment syndrome primarily relies on clinical assessment, and emergent intervention is needed before permanent visual loss occurs. CT imaging may aid in diagnosis in equivocal cases. Contrast-enhanced CT can demonstrate thrombosis or filling defects in the dilated superior ophthalmic vein, as observed in our case. Other findings of increased intraorbital pressure, such as proptosis, stretching of the optic nerve, posterior globe tenting, and retrobulbar fat stranding should be evaluated [8,9]. Besides identifying signs of increased intraorbital pressure, CT can help locate potential causes such as hematoma, emphysema, foreign bodies, or soft tissue expansion, which can guide further orbital decompression [8].

Conclusion

We described a rare complication of superior ophthalmic fat embolism and orbital compartment syndrome resulting from autologous fat grafting in the face. To prevent this complication, surgeons should perform the procedure with meticulous attention. Radiologists' awareness of this condition can facilitate timely diagnosis. Prompt detection, appropriate referral, and comprehensive multidisciplinary assessment are crucial for achieving favorable clinical outcomes.

THE ASEAN JOURNAL OF RADIOLOGY
ISSN 2672-9393

References

1. Cuzalina A, Guerrero AV. Complications in fat grafting. Atlas Oral Maxillofac Surg Clin North Am 2018;26:77-80. doi: 10.1016/j.cxom.2017.11.003.

2. Moellhoff N, Kuhlmann C, Frank K, Kim BS, Conte F, Cotofana S, et al. Arterial embolism after facial fat grafting: a systematic literature review. Aesthetic Plast Surg 2023;47:2771-87. doi: 10.1007/s00266-023-03511-y.

3. Dhooghe NS, Maes S, Depypere B, Claes KEY, Coopman R, Kubat B, et al. Fat embolism after autologous facial fat grafting. Aesthet Surg J 2022;42:231-8. doi: 10.1093/asj/sjab252.

4. Wang K, Rong X, Dang J, Yang J, Zheng H, Hou M, et al. Severe vascular complications caused by facial autologous fat grafting: a critical review. Ann Plast Surg 2021;86(3S Suppl 2):S208-S19. doi: 10.1097/SAP.0000000000002691.

5. Krastev TK, Beugels J, Hommes J, Piatkowski A, Mathijssen I, van der Hulst R. Efficacy and safety of autologous fat transfer in facial reconstructive surgery: a systematic review and meta-analysis. JAMA Facial Plast Surg 2018;20:351-60. doi: 10.1001/jamafacial.2018.0102.

6. Putthirangsiwong B, Vongsilpavattana V, Leelawongs S, Chanthanaphak E, Tunlayadechanont P, Chokthaweesak W. Superior ophthalmic vein embolism following forehead augmentation with autologous fat injection. Aesthetic Plast Surg 2022;46:450-5. doi: 10.1007/s00266-021-02414-0.

7. Cardenas-Camarena L, Bayter JE, Aguirre-Serrano H, Cuenca-Pardo J. Deaths caused by gluteal lipoinjection: what are we doing wrong? Plast Reconstr Surg 2015;136:58-66. doi: 10.1097/PRS.0000000000001364.

8. McCallum E, Keren S, Lapira M, Norris JH. Orbital compartment syndrome: an update with review of the literature. Clin Ophthalmol 2019;13:2189-94. doi: 10.2147/OPTH.S180058.

9. Nguyen VD, Singh AK, Altmeyer WB, Tantiwongkosi B. Demystifying orbital emergencies: a pictorial review. Radiographics 2017;37:947-62. doi: 10.1148/rg.2017160119.

THE ASEAN JOURNAL OF RADIOLOGY
ISSN 2672-9393

Classic Case

Calcific uraemic arteriolopathy: A rare but devastating complication of end-stage renal failure

Pak Lun LAM, FRCR[(1)]
Chi Hin CHAN, FHKAM (Radiology)[(1)]
Dicken WONG, FRCR[(1)]
Kwan Shun NG, FHKAM (Pathology)[(2)]
Danny Hing Yan CHO, FHKAM (Radiology)[(1)]
From [(1)]Department of Diagnostic and Interventional Radiology and
[(2)]Department of Pathology, Kwong Wah Hospital, Hong Kong.
Address correspondence to P.L.L. (e-mail: paklunlam@gmail.com)

Received 28 June 2024; revised 25 July 2024; accepted 12 August 2024
doi:10.46475/asean-jr.v25i2.897

Abstract

Calcific uraemic arteriolopathy is a rare complication of end-stage renal failure. It carries a grave prognosis with 1-year survival of under 50%. It occurs due to subcutaneous small vessel calcification, thrombosis, with subsequent tissue necrosis.

We described a case of calcific uraemic arteriolopathy in a 58-year-old man who presented with violaceous indurations over bilateral lower limbs, as well as large necrotic ulcer with adjacent eschars at the lower abdomen. Although skin biopsy is the gold standard for diagnosis, it is often avoided due to potential poor wound healing. On the other hand, in radiographs or computed tomography, fine linear or serpiginous subcutaneous calcifications are typical manifestations, which represent underlying small vessel calcifications. Radiological examinations, therefore, play an important role to establish the diagnosis.

Keywords: Calcific uraemic arteriolopathy, Calciphylaxis, Renal failure.

Background

Subcutaneous calcifications may often be dismissed, especially if there is significant pathology in the visceral organs or the skeletal structures. This article demonstrates a classic case of calcific uraemic arteriolopathy, a rare but serious complication of end-stage renal failure, which manifests as subcutaneous calcifications.

Case summary

A 58-year-old man was delivered to the emergency department in May 2023 with bilateral lower limb pain. He had morbid obesity, diabetes mellitus, and end-stage renal failure on peritoneal dialysis. Physical examination showed violaceous and plaque-like indurations over bilateral lower limbs, without open wound or signs of infection. Radiographs of bilateral lower limbs showed extensive subcutaneous fine linear calcific densities (Figure 1). He was discharged after the pain subsided with non-opioid analgesics.

In November 2023, he was admitted to the renal ward for blocked Tenckhoff catheter. A large necrotic ulcer with adjacent eschar was discovered at the left lower abdomen (Figure 2). The patient reported progressive pain and pruritis from his lower abdomen to bilateral lower limbs in the past month. He developed fever during his hospital stay, and computed tomography of the abdomen and pelvis was performed, showing subcutaneous small arteriole calcifications of the lower abdomen (Figure 3). While some calcified plaques were noted along the aorta, there were no extensive calcifications of the visceral organs, such as the kidneys, adrenals or pancreas (Figure 4). Clinical and radiological features were suggestive of calcific uraemic arteriolopathy. Wound swab showed multi-drug resistant Acinetobacter baumannii, and intravenous cefoperazone / sulbactam, metronidazole and minocycline were prescribed. Wound debridement was performed, and a histopathological examination of the excised skin tissue showed necrosis in the dermis and subcutis, as well as small vessel wall calcifications and thrombi, which were consistent with calcific uraemic arteriolopathy (Figure 5). Unfortunately, the patient deteriorated clinically, and succumbed due to multi-organ failure in one month.

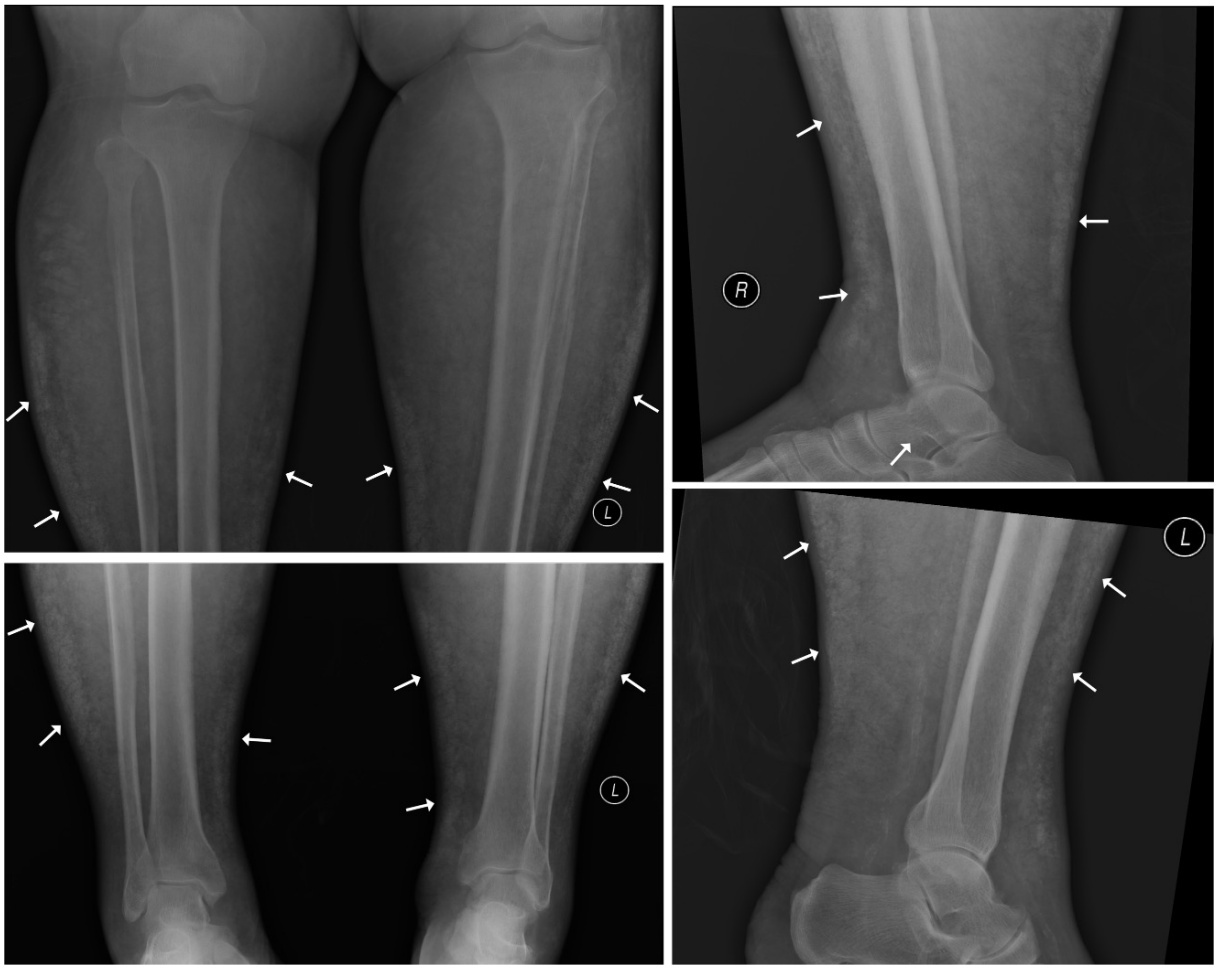

Figure 1. *Radiographs of the patient's bilateral lower limbs show extensive subcutaneous fine linear calcific densities (white arrows), suggestive of calcific uraemic arteriolopathy.*

Figure 2. *Image of the patient's left lower abdomen lateral and caudal to the Tenckhoff catheter insertion site shows a large 20cm x 15cm necrotic ulcer with adjacent eschar.*

THE ASEAN JOURNAL OF RADIOLOGY
ISSN 2672-9393

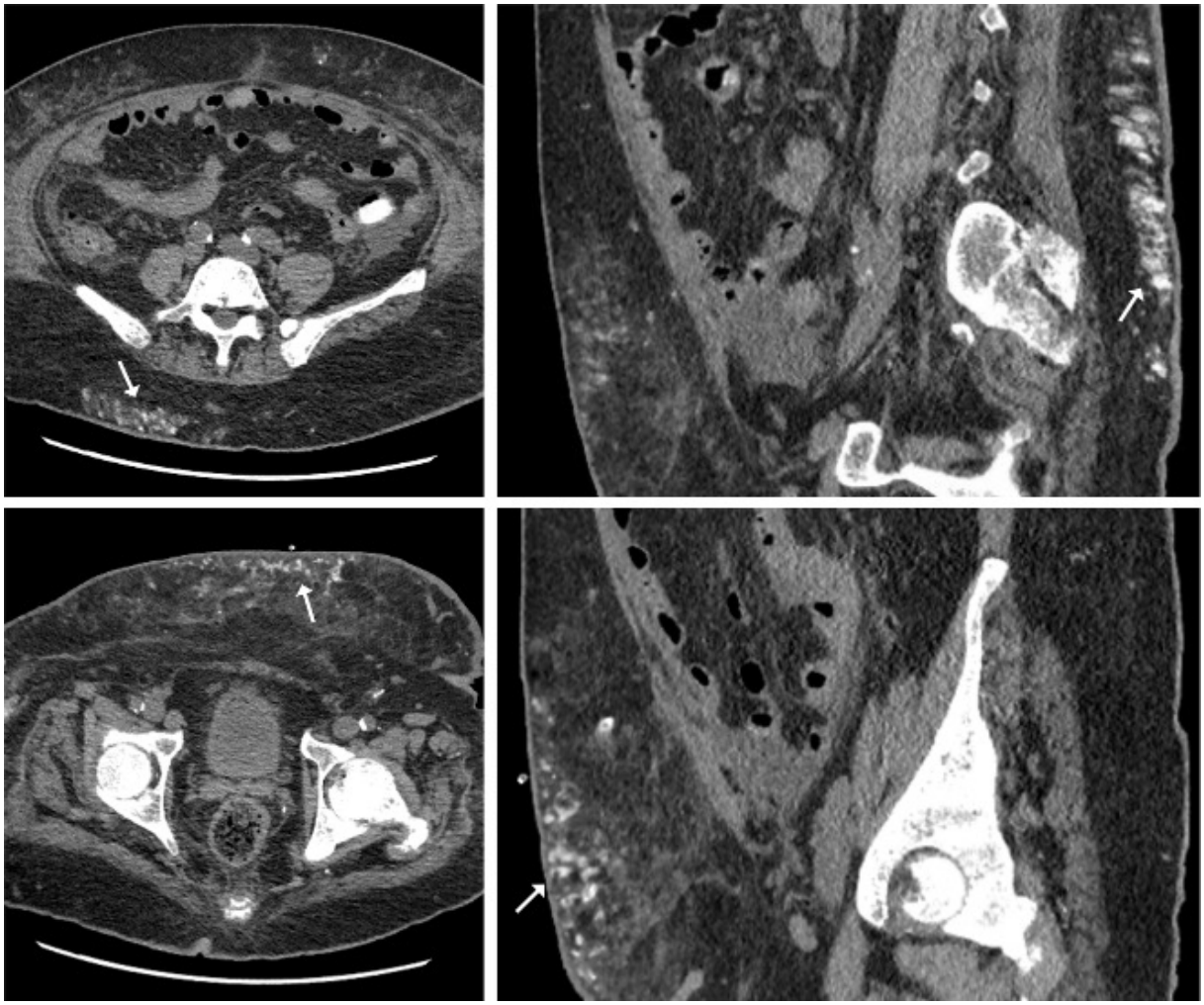

Figure 3. *Non-contrast computed tomography of the patient's abdomen and pelvis shows subcutaneous small arteriole calcifications of the lower abdomen (white arrows), suggestive of calcific uraemic arteriolopathy.*

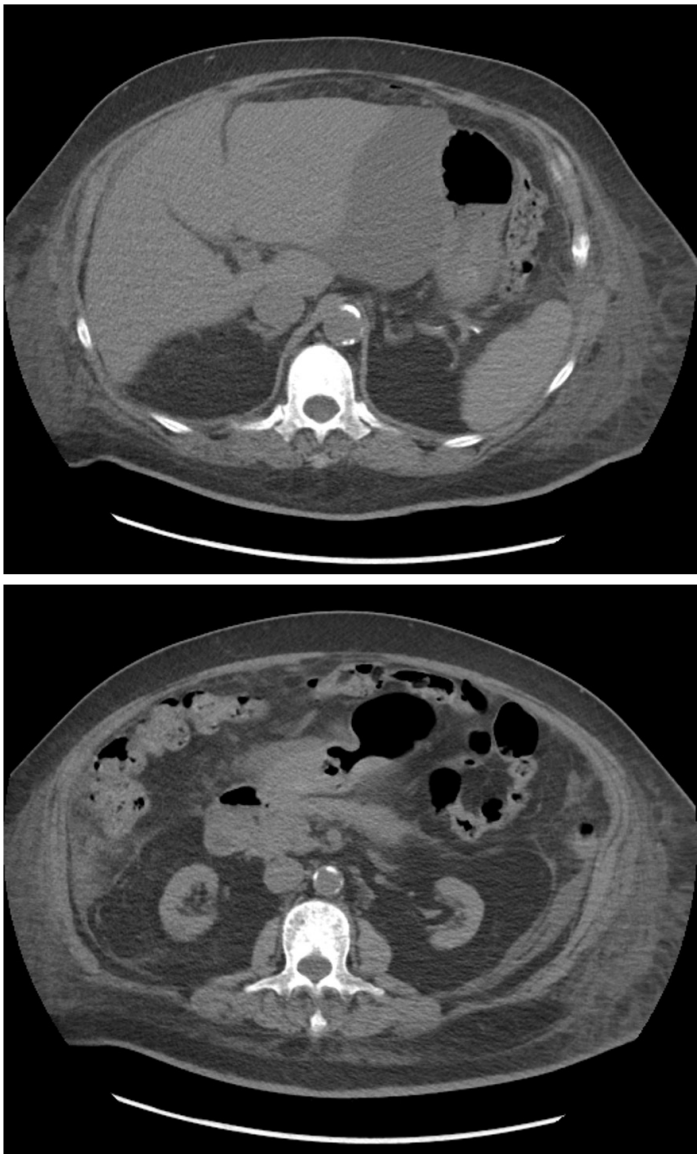

Figure 4. *Non-contrast computed tomography of the patient's abdomen and pelvis shows some calcified plaques along the aorta, though there are no extensive calcifications of the visceral organs, such as the kidneys, adrenals or pancreas.*

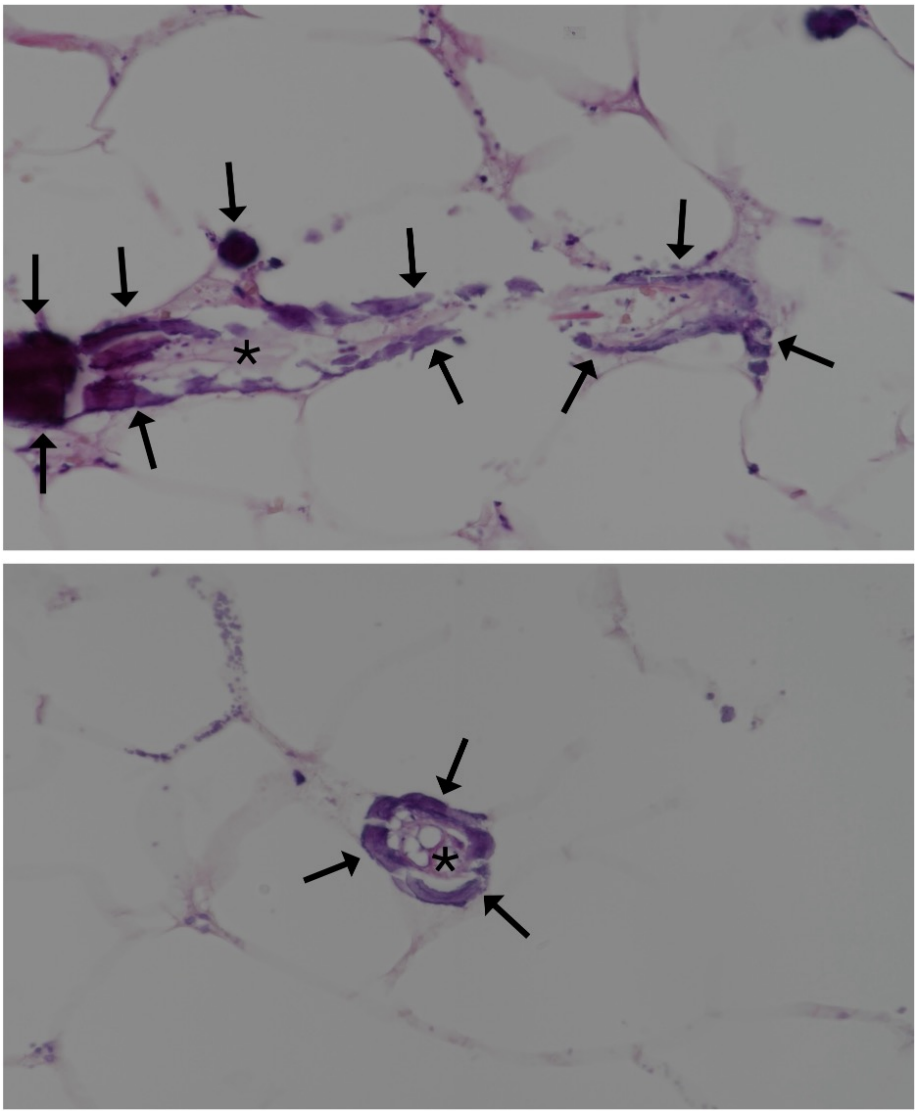

Figure 5. *Micrographs of the specimen (haematoxylin and eosin stain, 400x magnification) from debrided skin tissue from the patient's left lower abdominal wound show small vessel wall calcifications (black arrows) and thrombi (black asterisks), consistent with calcific uraemic arteriolopathy.*

Discussion

Calcific uraemic arteriolopathy, also known as calciphylaxis, is a rare complication of end-stage renal failure, occurring in less than 5% of patient on dialysis [1]. It carries a grave prognosis with 1-year survival of under 50% [2]. Its pathogenesis has yet been entirely elucidated, although hyperparathyroidism, deranged calcium and vitamin D levels, as well as chronic inflammation are postulated to play key roles. Risk factors include obesity, diabetes and female sex, the first two of which are present in this patient [2-3].

Calcific uraemic arteriolopathy typically presents with intense pain, pruritus and subcutaneous induration in the regions of greatest adiposity, more commonly in the lower limbs and the abdomen. It initially appears violaceous, which may eventually progress to eschars, and non-healing ulcers with cutaneous necrosis [1]. While it is usually diagnosed clinically, skin biopsy remains the gold standard. Histopathological examination usually shows small vessel calcification, endovascular fibrosis, thrombosis, as well as subcutaneous tissue necrosis [1-2]. Yet, skin biopsy is often avoided due to potential poor wound healing, especially when there is a superimposed infection. Radiological examinations, as illustrated in this case, are helpful to establish the diagnosis. In plain radiographs, fine linear subcutaneous calcifications are seen, which represent underlying small vessel calcifications. They are usually present in the lower limbs and the abdomen, corresponding to the symptomatic regions with skin and subcutaneous changes. Of note, this contrasts with tumoral calcinosis, another uncommon manifestation associated with chronic renal failure, which shows lobular calcified masses at periarticular locations with calcium sedimentation. Computed tomography can better delineate the distribution of calcification in small vessels, as well as exclude any presence of deep-seated infection [4-5].

There is no established treatment for calcific uraemic arteriolopathy in current literature. In view of a high infection risk, meticulous wound care and debridement of necrotic tissue are essential [2-4].

THE ASEAN JOURNAL OF RADIOLOGY
ISSN 2672-9393

To conclude, calcific uraemic arteriolopathy is a rare but devastating complication in patients with end-stage renal failure. It has distinctive radiological features which can help establish the diagnosis.

Ethics approval

The patient was treated in accordance with the Declaration of Helsinki. He provided informed consent for all treatments and procedures. The patient's next-of-kin provided informed consent for publication.

Conflicts of interest and source of funding

All authors declared no conflicts of interest. This research received no specific grant from any funding agency in the public, commercial, or not-for-profit sectors.

References

1. Colboc H, Moguelet P, Bazin D, Carvalho P, Dillies AS, Chaby G, et al. Localization, morphologic features, and chemical composition of calciphylaxis-related skin deposits in patients with calcific uremic arteriolopathy. JAMA Dermatol 2019;155:789-96. doi: 10.1001/jamadermatol.2019.0381.

2. Weenig RH, Sewell LD, Davis MD, McCarthy JT, Pittelkow MR. Calciphylaxis: natural history, risk factor analysis, and outcome. J Am Acad Dermatol 2007; 56:569-79. doi: 10.1016/j.jaad.2006.08.065.

3. Jovanovich A, Chonchol M. Calcific uremic arteriolopathy revisited. J Am Soc Nephrol 2016;27:3233-5. doi: 10.1681/ASN.2016040480.

4. Jeong HS, Dominguez AR. Calciphylaxis: controversies in pathogenesis, diagnosis and treatment. Am J Med Sci 2016;351:217-27. doi: 10.1016/j.amjms. 2015.11.015.

5. Bleibel W, Hazar B, Herman R. A case report comparing various radiological tests in the diagnosis of calcific uremic arteriolopathy. Am J Kidney Dis 2006; 48:659-61. doi: 10.1053/j.ajkd.2006.05.031.

THE ASEAN JOURNAL OF RADIOLOGY
ISSN 2672-9393

ASEAN Movement in Radiology

Value-based radiology in Asia-Oceania: Current status and future directions

Evelyn Lai Ming Ho, MBBS, MMed[(1), (2)]
Joseph KT Lee, MD, FACR[(3)]
Cher Heng Tan, MBBS, FRCR, [(4), (5)]
From [(1)]Immediate Past President (2023-2025), Asian Oceanian Society of Radiology (AOSR),
[(2)]Imaging Department, ParkCity Medical Centre Kuala Lumpur, Malaysia,
[(3)]Department of Radiology, University of North Carolina (UNC) at Chapel Hill, USA,
[(4)]Department of Diagnostic Radiology, Tan Tock Seng Hospital, Singapore,
[(5)]Lee Kong Chian School of Medicine, Nanyang Technological University, Singapore.
Address correspondence to E.L.M.H. (e-mail: evelynlmho@gmail.com)

Received 22 June 2024; revised 22 August 2024; accepted 23 August 2024
doi:10.46475/asean-jr.v25i2.915

Keywords: Value-based radiology, VBR, AOSR, Leadership, Communications.

The Asian Oceanian Society of Radiology (AOSR) is primarily a federation of 24 radiological organizations from Asia-Oceania (https://theaosr.org) with varied cultures, languages, population sizes, country-land areas, economies, and geopolitics. AOSR has no low-income country members [World Bank] [1]. The AOSR is made up of 10 lower-middle-income [1] (LMIC), 5 upper-middle-income [1] (UMIC) and 9 high-income [1] territory/country radiological societies and a few individual members. Radiology has been recognized as a contributor to increasing healthcare costs and must work towards reducing low-value care [2,3]. The understanding and practice of VBR is diverse amongst the AOSR society members [4], ranging from not being aware of the term to those who practice it [5].

In 2021, the AOSR leadership participated in the International Society for Strategic Studies in Radiology value-based radiology (VBR) strategic planning workshops. This provided (or proved to be) the impetus for the AOSR to formulate an action plan for advancing VBR in our region.

2022-2024: VBR Survey-Webinar-Workshop

2022 VBR Survey

The AOSR value-based radiology (VBR) survey was conducted from May 5th to June 30th, 2022, to assess the extent to which VBR was practiced and barriers encountered. The feedback on the survey was encouraging. For those who had not considered VBR, they were now aware, and interested in learning more about it whilst comments from open-ended questions provided useful insights.

The survey questions in English were approved by the AOSR Councilors and converted to an online Google Form. The AOSR office emailed the online survey link to member societies' administrative offices for distribution to their membership. For those with limited access to the Google form, they could respond to the survey in Microsoft Word document. Those responding on behalf of a radiological organization were to answer as objectively as possible to reflect their respective practices. As this was also meant to generate VBR awareness, there was no limitation on the number of respondents, even if they came from the same center of practice. Responses were accepted from any individual in the region.

The survey questions pertained to clinical practice of multidisciplinary teams (MDTs), reducing duplicate and redundant follow-up examinations, appropriate use criteria (AUC), a clinical decision support system (CDSS), key performance indicators (KPIs) to measure patient outcomes related to modalities and procedures, and communications with various stakeholders.

Questions were designed in a "yes or no" format, on a Likert scale or with free text answers covering four domains: barriers to establishing MDTs, systems preventing duplicate/redundant examinations, KPIs for patient outcomes and provision of lay language reports to patients. Respondents were contacted for clarifications, if their answers were ambiguous or for those from the same centers with apparently incongruous answers.

Table 1: Respondents Territory/Country Distribution

Territory/Country	No. of Respondents
High Income	
Australia	2
Chinese Taipei	1
Hong Kong SAR	4
Japan	4
Oman	1
Singapore	1
South Korea	2
Upper-Middle-Income	
Indonesia	8
Kazakhstan	1
Malaysia	1
Thailand	1
Lower-Middle-Income	
Bangladesh	3
India	3
Mongolia	1
Myanmar	11
Papua New Guinea	1
Philippines	1
Uzbekistan	1
Vietnam	1
Total	**48**

Respondents were informed that the report of the survey findings would be on the condition of anonymity apart from their region/country of origin. The survey results were tabulated on Microsoft Excel. No statistical analysis was required, as this was primarily a cross-sectional study of prevalence of practice patterns.

There were 48 respondents (45 senior and 2 junior radiologists, 1 resident) from 19 different countries/regions/territories (Table 1). Fifteen were from high-income (HIC), 11 from upper middle-income (UMIC) and 22 from lower-middle-income countries/territories/regions (LMIC). Eighteen of our 24 radiological societies participated in the survey. The countries/regions/territories represented about 2.58 billion people in 2022 (https://www.worldometers.info/world-population/). Six responded on behalf of their societies. Respondents were from a variety of institutions – government, academic, private centers and were located in cities or larger towns.

Survey findings indicated variable VBR awareness, understanding and practice amongst AOSR members (Table 2). Many respondents worked in practices that had MDTs, collaborating with various medical specialties with the majority serving to understand each other's needs. Only about half of the respondents (about half each as well within HICs and LMICs) had systems in place to prevent duplicate and redundant follow-up examinations. Access to imaging was available within the center but dropped dramatically once it was outside the center.

Table 2: AOSR Value-based Radiology Survey Results Summary

Multidisciplinary Teams (MDTs)	**Yes**	**No**	**Total**
Your practice has MDTs involving radiologists, referring practitioners and other relevant personnel to:			
Understand each other's needs	45 (94%)	3 (6%)	48 (100%)
Improve response to gaps in healthcare management	35 (73%)	13 (27%)	48 (100%)
Optimize utilization of existing resources	35 (73%)	13 (27%)	48 (100%)
Develop resources of the future	30 (63%)	18 (38%)	48 *(101%)
Preventing Duplicate and Redundant Follow-up Examinations			
There are systems in place to prevent duplicate or redundant follow-up examinations in your department/center or region or country. If yes, please answer the following:	23 (48%)	25 (52%)	48 (100%)
There is access to patient imaging and reports within a center	23 (100%)	0 (0%)	23 (100%)
There is access to patient imaging and reports within a state/region of the country	11 (48%)	12 (52%)	23 (100%)
There is access to patient imaging and reports within the country	10 (43%)	13 (57%)	23 (100%)
Patients have a record book to log their examinations	10 (43%)	13 (57%)	23 (100%)
There are other systems in place for reducing duplicate or redundant examinations. If the answer was yes, briefly state what these systems were [1]:	7 (30%)	16 (70%)	23 (100%)
Appropriate Use Criteria (AUC)			
Does your center use any form of AUC to guide selection of the most appropriate imaging examination to answer the clinical question? If yes, give details [2]:	22 (46%)	26 (54%)	48 (100%)
Do you involve non-radiologist clinicians/specialists in developing AUC including 'no need to image'?	31 (65%)	17 (35%)	48 (100%)
Clinical Decision Support System (CDSS)			
Does your center use any form of CDSS? If yes, please elaborate briefly [3]:	3 (6%)	45 (94%)	48 (100%)
Key Performance Indicator/s (KPIs) that measure patient outcomes in relation to modalities and procedures			
Do you work with or are you aware of healthcare stakeholders working with imaging industry partners to develop software/apps that gather information on KPIs? If yes, please give brief details [4]:	8 (17%)	40 (83%)	48 (100%)
Will you be interested to work with your non-radiology colleagues to develop KPIs?	45 (94%)	3 (6%)	48 (100%)

	****Agree**	**Neutral**	****Disagree**	**Total**
Key stakeholders should work with imaging industry partners to develop relevant KPI software	34 (71%)	11 (23%)	3 (6%)	48 (100%)
At equipment purchase, there should be appropriate training related to deployment and interpretation of information provided by the KPI software	39 (81%)	5 (10%)	4 (8%)	48 *(99%)
Communications and Lay Language Reports				
There should be training to enable radiologists to improve the ability to communicate with patients	40 (83%)	3 (6%)	5 (10%)	48 *(99%)
There should be training to enable radiologists to improve the ability to communicate to mass media	34 (71%)	11 (23%)	3 (6%)	48 (100%)
There should be a specially designated person/s for communication with mass media	41 (85%)	3 (6%)	4 (8%)	48 *(99%)
Research on direct patient communication is important even in radiology	40 (84%)	5 (10%)	3 (6%)	48 (100%)
A tool/apps developed to provide patients with disease/imaging specific information is important	38 (79%)	8 (17%)	2 (4%)	48 (100%)
A tool/apps developed to provide patient-friendly decision support will improve radiology-patient interactions and understanding of what imaging/procedure is most appropriate	38 (79%)	8 (17%)	2 (4%)	48 (100%)
Patients should have access to their imaging/procedure reports in lay language	20 (42%)	15(31%)	13 (27%)	48 (100%)

	Yes	**Do not know or not sure**	**No**	**Total**
There is a specially designated person/s within your radiology organization/center for communication with mass media	17 (35%)	11(23%)	20 (42%)	48 (100%)
There is research on direct patient communication in your center/area/region/country?	9 (19%)	14 (29%)	25 (52%)	48 (100%)

*Rounding reason; **sum of the strongly agree/agree and strongly disagree/agree responses

1. A central clinical management system with a pop-up prompt once it detected duplicate inputs within a specified time frame requiring a reason for the order entry; national health insurance system that required pre-approval; hospital management cost and quality control team decision; scheduling and archive comparison.

2. 14 were clinical and other referral guidelines (developed in-house, own health ministry, own professional body), local and foreign (American College of Radiology, European Society of Radiology, National Comprehensive Cancer Network, National Institute for Care and Excellence, neighbouring country); 3 were specific clinical presentations and/or departments for example in ER, for stroke & backpain; 4 were related to vetting each request for appropriateness: short interview with patients/check logbook, vetting requests to make decision on appropriate imaging, direct discussion with radiologist; 1 did not give further details.

3. Artificial intelligence CDSS tool for stroke and specific disease conditions which informs both radiologists and referring physicians to aid in diagnosis and treatment

4. Collection of KPIs (such as turnaround time, stroke outcome) by government hospital network, use of the ACR as reference, use of commercial software (RadimetricsTM), and development within a university AI department.

THE ASEAN JOURNAL OF RADIOLOGY
ISSN 2672-9393

Overall, nearly half of the respondents used any form of AUC: 40% HIC, 45% UMIC, 50% LMIC. A few respondents considered personally vetting for appropriateness, a form of AUC. Most of the others used locally developed clinical practice guidelines, established foreign guidelines or a combination of the two. An overwhelming majority of our respondents did not have any CDSS integrated into the radiology order entry system.

Only a fifth of respondents were aware of or working with industry partners to develop software applications that gather KPIs for measuring patient outcomes related to modalities and procedures. However, an overwhelming majority indicated interests in working with non-radiology colleagues to develop such software. Most of the respondents agreed that key stakeholders should work with imaging industry partners to develop relevant KPIs and that there should be appropriate training at the time of equipment purchase for deployment and interpretation of the KPIs.

Factors like manpower shortage, lack of money and time, restrictive policies including data privacy laws and lack of unified national policies, self-centered physician behaviors as well as poor communications between stakeholders and poor patient compliance, were consistently mentioned as barriers across the domains surveyed (establishment of MDTs, usage of KPIs for patient outcomes and reduction of duplicate examinations).

For MDTs, other barriers were the lack of incentives from hospital administration for non-interpretive activities and the lack of interest and teamwork training amongst physicians. Many were skeptical about the use of KPIs, as it was perceived as an imperfect tool that could create conflicts among healthcare professionals.

The absence of and deficiencies in information technology (IT) were cited as major barriers to prevent duplicate examinations. Incompatible systems and privacy laws prevented cross-accessibility. Physicians' failure to review available records required additional pop-up alerts in the order entry system. Patients who registered with different names confounded the problem. In manual systems,

physicians' failure to take a complete history and patients' inability to keep track of even their own logbook were other factors. Another detractor was the radiologists' lack of authority in denying seemingly duplicate or redundant examinations in some regions.

For some of our respondents, an insurance system that required pre-approval helped reduce duplicate and redundant examinations. However, such an insurance system could result in denial of legitimate urgent requests if the same imaging modality was requested within a defined time period, even if it was meant for different anatomical regions or clinical indications. Such system imperfection had resulted in user dissatisfaction and led physicians to seek ways to bypass the system.

The respondents agreed with the importance of research in direct patient communication and had a high level of interest in improving their skills in communicating with patients. While many also acknowledged the importance of engaging mass media, most preferred a specially designated person for this function. Many also agreed it was important to develop digital applications with disease/imaging specific information to improve radiology-patient interactions and allow patients to understand the most appropriate imaging/procedure for their conditions.

Respondents were ambivalent about the provision of lay language reports to patients with less than half agreeing to the idea regardless of their country's economic status or their level of agreement when asked to give their comments. A few respondents indicated that directly talking to the patients about their findings could obviate a lay language report especially where the reporting language and the spoken languages were different.

Reasons in support of lay language reports were broadly categorized into 'patients' right to a report in a language they could understand' and 'improved patient outcomes'. Better patient outcomes might result from a better understanding of their condition, timely access that allayed patient anxiety and improved patient

THE ASEAN JOURNAL OF RADIOLOGY
ISSN 2672-9393

satisfaction with overall better compliance especially for those needing to travel great distances to urban centers to seek medical treatment.

Reasons against the use of lay language reports were possible poorer patient outcomes, increased medicolegal risks and heavier radiologist workload from providing 2 reports per patient. Reduced report accuracy as a result of oversimplification and imprecise translation into the vernacular language raised the fear of medicolegal risks. A lay language report with complex findings or a diagnosis of malignancy may cause undue anxiety that might otherwise have been tempered during consultation with their primary physician. Patient outcomes might also be worse if they misunderstood their lay language report and decided to self-treat, sought alternative medicine, and defaulted follow-up, which might lead to radiologist with referring non-radiologist physician conflict.

The data from the survey is small with a skewed sample size. The AOSR also could not dictate how each society member promoted the survey to its own membership. As the survey was in English, only those proficient in English responded whilst some responses were from society leadership only. Most of the respondents were also from urban hospitals.

There was an initial attempt to see if there were differences in responses from LMICs and HICs but these were not significant because of the small and skewed sample size. Anecdotally, unexpected findings were in the level of agreement to provide lay language reports and a similar lack of a system to reduce duplicates or that proportionately more of LMICs seemed to have some form of AUC compared to HICs. These seeming discrepancies may be related to how having IT systems does not automatically help reduce duplicates, and also on how each respondent defined AUC. HICs might consider AUC as specific software, whilst manual systems amongst LMICs were considered a form of AUC. Commonalities highlighted were the relationship of the radiologist with the non-radiologist physician as well as communication difficulties with perceived or real inabilities for the radiologist to be heard and respected. Such insights from the information provided the AOSR guideposts to chart the next steps.

2023 The Connected Radiologist Webinar

To this end, a webinar was organized in January 2023 on how to be confident beyond the radiology reporting room, promoting communication and collaboration of radiologists with other medical disciplines, patients and having meaningful community engagement. Dr Chantsalsuren Galbaatar, spoke on 'Engaging Colleagues in Medicine', giving her experience on how she juggled time as a radiologist and led the activities as CEO of the Mongolian Medical Women's Association. Dr Geraldine McGinty, a past American College of Radiology president spoke on 'The Visible Radiologist' whilst Dr Angelica Robinson from University of Texas shared her experience and "how to" on community engagement in her talk on 'Captivating Communicator'. A guest panelist Dr Charles Goh from Singapore joined the discussion. The webinar ended with a very robust panel discussion.

Feedback was encouraging with 78% and 22% stating the webinar was very useful and useful, respectively. There were 246 registrations and 101 who attended live, mostly from 11 countries/region in Asia-Oceania as well as a handful of attendees from Lithuania, Saudi Arabia and Portugal.

THE ASEAN JOURNAL OF RADIOLOGY
ISSN 2672-9393

2024 VBR Track and Workshop: Radiology Leadership Intensive: 'How to Lead the Way in Becoming a Visible Radiologist?'

At the recently concluded Asian Oceanian Congress of Radiology 2024 (AOCR2024) in March, Taipei, a VBR track with didactic lectures followed by a breakout session with small groups and ensuing wrap up session was conducted. The AOSR recorded its appreciation to Dr Geraldine McGinty and Dr Frank J. Lexa for leading the way in this track and workshop. 'Why every radiologist must be a leader', 'Negotiations – it's more than just money' and 'Speaking up and leading change without being seen as a troublemaker' were the focus. For the breakout sessions, participants were given scenarios to play out and discuss.

The various small groups regrouped for a wrap up session and discussion followed by a group photo for memories of a very productive workshop.

What Next? Future Directions

One of our favorite quotes is attributed to Lao Tzu, 'The Journey of a Thousand Miles Begins with A Single Step'. Without labelling our activities as such, we had already taken our first steps into VBR. In 2021, the AOSR Emerging Trends Committee embarked on developing and adopting disease specific structured reporting templates in more than 1 language (soon to be available on https://theaosr.org/) amongst the membership to ensure the patient's results would be communicated consistently and provided all the essential information to the management care team. AUCs should be promoted and multidisciplinary development of AUCs encouraged.

In the same year, AOSR officially launched AsiaSafe [6] with its website https://asiasafe.org/. AsiaSafe originally started with a vision for building a radiation safety culture but early on had its mandate extended to other aspects of safety including MR safety and even contrast safety. Both of these ventures ensure better outcomes for the patient – adding value to radiology and healthcare in our region.

After the 2022 AOSR VBR survey, the results of the survey were shared with the society membership through the AOSR President's Roundtable. Despite the cultural differences, widely varying resources and language differences, it was agreed that all could improve communication skills with patients and other stakeholders in healthcare, and even amongst the other members within an MDT. A train-the-trainers for leadership and communications might be an area to work on, so that these can be replicated in the various languages of each territory/region and have a wider reach. Consistent and persistent efforts which are resource stratified and practical in our region will be needed. In the meantime, a VBR track is in the pipeline for the AOCR2025 (Chennai, India) in January 2025.

Our revamped AOSR website https://theaosr.org/ in 2024, would also be useful for promoting and sharing resources and ideas. We hope that through our various efforts, AOSR can assist the radiology communities within the Asian-Oceanian region to develop future thought leaders, who will contextualize global best practices to be implemented in their respective health systems, and thereby increase the value of radiology and radiologists.

Acknowledgements

The authors thank the present and past executive councilors of the AOSR for their support, commitment, and efforts; all who participated in the survey; our friends of the AOSR- Dr Geraldine B. McGinty and Dr Frank J. Lexa who were our VBR track and workshop speakers/facilitators; the speakers/panelists who participated in the 2023 communications webinar as well as the organizing committees of the AOCR2024 and AOCR2025 for incorporating the VBR tracks.

THE ASEAN JOURNAL OF RADIOLOGY
ISSN 2672-9393

References

1. Our World in Data [Internet]. 2023 [cited 2024 Aug 21]. World Bank income groups. Available from: https://ourworldindata.org/grapher/world-bank-income-groups

2. Brady AP, Bello JA, Derchi LE, Fuchsjäger M, Goergen S, Krestin GP, et al. Radiology in the era of value-based healthcare: a multi-society expert statement from the ACR, CAR, ESR, IS3R, RANZCR, and RSNA. Radiology [Internet]. 2021 [cited 2024 Aug 21]; 298:486–91. Available from: https://pubs.rsna.org/doi/10.1148/radiol.2020209027

3. European Society of Radiology (ESR). Value-based radiology: what is the ESR doing, and what should we do in the future?. Insights Imaging [Internet]. 2021 [cited 2024 Aug 21]; 12:108. Available from: https://insightsimaging.springeropen.com/articles/10.1186/s13244-021-01056-9

4. European Society of Radiology (ESR). Summary of the proceedings of the International Forum 2018: "Value-based radiology". Insights Imaging [Internet] 2019 [cited 2024 Aug 21]; 10:34. Available from: https://insightsimaging.springeropen.com/articles/10.1186/s13244-019-0717-7

5. Jeon SK, Kim SH, Shin CI, Yoo J, Park KJ, Ryoo SB, et al. Role of dedicated subspecialized radiologists in multidisciplinary team discussions on lower gastrointestinal tract cancers. Korean J Radiol [Internet]. 2022 [cited 2024 Aug 21];23:732-41. Available from: https://kjronline.org/DOIx.php?id=10.3348/kjr.2021.0680

6. Ho ELM, Ng KH. AsiaSafe: Cultivating a safety culture for radiation in diagnosis, intervention, therapy, and beyond. Korean J Radiol [Internet]. 2024 [cited 2024 Aug 21];25:8-10. Available from: https://kjronline.org/DOIx.php?id=10.3348/kjr.2023.0945

THE ASEAN JOURNAL OF RADIOLOGY
ISSN 2672-9393

Letter to the Editor and Reply

Subclinical tuberculosis

Received 18 July 2024; revised 21 July 2024; accepted 22 August 2024
doi:10.46475/asean-jr.v25i2.919

We read with great interest the article "Tuberculosis: Important lessons from AOCR 2023, Bangkok, Thailand" by Pakkal M, et al., published in The ASEAN Journal of Radiology (2023; 24(2): 180-198). We congratulate and thank the authors for their insightful summary of the current state and imaging advancements in tuberculosis (TB) across various societies. Here, we would like to make some contributions and expand on the discussion by sharing our viewpoints on the emerging TB continuum concept and the crucial role of imaging in TB control.

First and foremost, the article's discussion on the new concept of the TB spectrum, including subclinical TB, is highly commendable. Subclinical TB is a significant concern as it may be a major contributor to TB transmission due to its asymptomatic nature and potential for spreading the pathogen [1]. Most individuals with subclinical TB are detected through screening approaches, particularly chest X-rays (CXR). For example, recent work at a university hospital in Bangkok, Thailand, showed that the majority (69.2%) of healthcare workers with pulmonary TB from 2018-2022 were subclinical and mainly detected through routine health checks [2]. Additionally, data from the same hospital found that 22.2% to 29.8% of such cases had positive culture results, implying that roughly a quarter of individuals with subclinical TB may be contagious [2,3]. Importantly, diagnosing subclinical TB enables early treatment initiation, preventing further TB transmission within the community.

Second, we would like to address the use of the term "incipient TB" in Figure 6, which is intended to depict the radiologic progression of TB. Incipient TB refers to a transitional stage of TB infection that precedes subclinical and active TB disease. However, there is currently no clear diagnostic method for identifying incipient TB, and its definition remains ambiguous. According to Drain PK et al., incipient TB does not show radiographic abnormalities or microbiologic evidence [4]. In this case, a small nodule observed on CT (Figure 6C) may be retrospectively

considered incipient TB, which later progressed to subclinical TB, as depicted in Figure 6D. Noteworthily, Yoon et al. provided an interesting visualization of this new concept of the TB spectrum [5].

Third, subclinical TB, an early stage of the disease, often presents less severe radiologic abnormalities [6]. We agree with the article's endorsement of computer-aided diagnosis (CAD) as a valuable tool for TB screening and triage. However, it is important to note that deep learning models developed using data from one population may perform differently in another [7]. Furthermore, the proportion of subclinical TB cases in the training dataset may still be uncertain. As a result, including subclinical TB cases, particularly from local populations, in the training dataset is necessary for effectively developing deep-learning models for TB screening.

Fourth, we found the article's reference to various imaging modalities for TB diagnosis particularly compelling. From our experience, LDCT facilitates earlier TB diagnosis, especially in subclinical cases. Low-dose CT (LDCT) improves diagnostic accuracy while offering lower radiation exposure compared to conventional-dose CT. At our center, individuals typically undergo CXR as part of routine health checks, and those with abnormal findings are referred to chest physicians within the health check service. Patients with equivocal radiographic findings often receive an LDCT scan on the same day to aid in diagnosis as appropriate. Given the availability of CT, we support utilizing LDCT in such cases to reduce diagnostic delays.

In conclusion, emphasizing the modern concept of the TB spectrum in symposia underscores the commitment to the end-TB movement. Indeed, radiology plays a key role in diagnosing TB disease. We advocate that prioritizing subclinical TB is immensely important for TB control, and detecting and treating TB at this stage could be highly beneficial. In addition, we thereby believe it is crucial to revisit the policy on using CXR for widespread TB screening in countries with high burdens of TB. Research and collaborative efforts among clinical, radiology, and public health sectors are vital for tackling the TB epidemic and ultimately achieving its eradication.

THE ASEAN JOURNAL OF RADIOLOGY
ISSN 2672-9393

Supakorn Chansaengpetch, M.D.[(1)]
Narongpon Dumavibhat, M.D., Ph.D.[(1), (2)]
From [(1)]Department of Preventive and Social Medicine, Faculty of Medicine Siriraj Hospital, Mahidol University, Thailand.
[(2)]Siriraj Tuberculosis Comprehensive Center, Siriraj Hospital, Bangkok, Thailand
Address correspondence to N.D. (e-mail: dumavibhat@yahoo.com)

Conflict of Interest

None declared.

References

1. Kendall EA, Shrestha S, Dowdy DW. The epidemiological importance of subclinical tuberculosis. a critical reappraisal. Am J Respir Crit Care Med 2021;203:168–74. doi: 10.1164/rccm.202006-2394pp.

2. Virojskulchai T. Incidence and characteristics of subclinical and active pulmonary tuberculosis among healthcare workers at a university hospital [dissertation]. Bangkok: Mahidol University; 2024.

3. Chansaengpetch S, Kaewlai R, Virojskulchai T, Jaroonpipatkul A, Chierakul N, Muangman N, et al. Characteristics of culture-negative subclinical pulmonary tuberculosis: a single-center observation. Multidiscip Respir Med 2024;19:955. doi: 10.5826/mrm.2024.955.

4. Drain PK, Bajema KL, Dowdy D, Dheda K, Naidoo K, Schumacher SG, et al. Incipient and subclinical tuberculosis: a clinical review of early stages and progression of infection. Clin Microbiol Rev 2018;31:e00021-18. doi: 10.1128/cmr.00021-18.

5. Yoon SH, Goo JM, Yim JJ, Yoshiyama T, Flynn JL. CT and 18F-FDG PET abnormalities in contacts with recent tuberculosis infections but negative chest X-ray. Insights Imaging 2022;13:112. doi: 10.1186/s13244-022-01255-y.

6. Jeong YJ, Park JS, Kim HW, Min J, Ko Y, Oh JY, et al. Characteristics of subclinical tuberculosis compared to active symptomatic tuberculosis using nationwide registry cohort in Korea: prospective cohort study. Front Public Health 2023;11:1275125. doi: 10.3389/fpubh.2023.1275125.

7. Sathitratanacheewin S, Sunanta P, Pongpirul K. Deep learning for automated classification of tuberculosis-related chest X-Ray: dataset distribution shift limits diagnostic performance generalizability. Heliyon 2020;6:e04614. doi: 10.1016/j.heliyon.2020.e04614.

The author replies:

I read with great interest the Letter to the Editor by Chansaengpetch and Dumavibhat regarding my publication "Tuberculosis: Important lessons from AOCR 2023, Bangkok, Thailand."

One of the main goals of my presentation was to discuss the situation and the role of radiology in tuberculosis.

First, I agree that most individuals with asymptomatic TB are detected through screening tools, especially chest X-ray (CXR). I commend the authors' finding that among healthcare workers who developed pulmonary tuberculosis from 2018 to 2022, the majority (69.2%) had subclinical tuberculosis. We also showed that 97 of the 8,044 cohort participants experienced spontaneous healing from latent tuberculosis, as confirmed by chest X-ray (CXR) [1].

Second, as noted in the commentary by Chansaengpetch and Dumavibhat, it is known that patients diagnosed with incipient TB may benefit from early intervention to prevent progression to active tuberculosis [2]. Indeed, incipient TB is an ambiguous concept as it encompasses a spectrum of different stages that may or may not progress to active TB. Incipient TB does not show radiographic abnormalities or microbiologic evidence. CT stands out as a more sensitive imaging modality compared to CXR when it comes to identifying parenchymal lesions associated with incipient TB. Yoon et al. noted that advanced imaging tools such as CT and 18-fluorodeoxyglucose PET may help further stratify individuals intensely exposed to M. tuberculosis on a continuous spectrum from latent tuberculosis to incipient, subclinical, and active tuberculosis [3].

Third, I fully agree with the opinion that including subclinical TB cases, especially those from local populations, in training datasets is essential for effectively developing deep learning models for TB screening.

Fourth, CT is significantly superior to CXR in consistently identifying TB, especially subclinical TB. Low-dose CT could be used as an alternative to standard-dose CT for the detection of latent TB. Digital tomosynthesis (DTS) can offer a reasonable option for detecting lung lesions in individuals who have had contact with TB patients [4]. The imaging modalities for screening ITB or latent TB may vary depending on the circumstances of each country. For example, since the cost of DTS is lower than that of CT, DTS may be preferred over CT in some cases.

Overall, we appreciate and concur with Chansaengpetch and Dumavibhat's opinion. Additionally, further prospective studies are needed to better define incipient tuberculosis.

Ki Yeol Lee, M.D., Ph.D.
From Department of Radiology, Korea University Guro Hospital, South Korea.
Address correspondence to K.Y.L. (e-mail: cornerstonelee@gmail.com or kiylee@korea.ac.kr)

References

1. Rotundo S, Tassone MT, Serapide F, Russo A, Trecarichi ET. Incipient tuberculosis: a comprehensive overview. Infection 2024;52:1215-22. doi: 10.1007/s15010-024-02239-4.

2. Moore N, Maher M, Murphy G, O'Callaghan Maher M, O'Connor OJ, McEntee MF. CT detection in the detection of latent tuberculosis: a systematic review. Clin Radiol 2023;78:568-75. doi: 10.1016/j.crad.2023.04.014.

3. Yoon SH, Goo JM, Yim JJ, Yoshiyama T, Flynn JL. CT and 18F-FDG PET abnormalities in contacts with recent tuberculosis infections but negative chest X-ray. Insights Imaging 2022;13:112. doi: 10.1186/s13244-022-01255-y.

4. Mok J, Yeom JA, Nam SW, Yoo JM, Lee JW, Lee G, et al. Role of digital tomosynthesis in the context of tuberculosis contact investigation: comparisons with digital radiography. Acta Radiol 2022;63:901-8. doi: 10.1177/02841851211022498.

ASEAN JOURNAL OF RADIOLOGY

This journal provide 4 areas of editorial services: language editing, statistical editing, content editing, and complete reference-citation check in 8 steps:

Step	Services to authors	Services providers
I	Manuscript submitted	Editor
II	Language editing/ A reference-citation check	Language consultant/Bibliographer
III	First revision to ensure that all information remains correct after language editing	Editor
IV	Statistical editing	Statistical consultant
V	Content editing*	Three reviewers
VI	Second revision	Editor
VII	Manuscript accepted/ rejected	Editor/Editorial board
VIII	Manuscript published	Editorial office

*Content editing follows a double-blind reviewing procedure